On Error Estimates of an Exponential Wave Integrator Sine Pseudospectral Method for the Klein–Gordon–Zakharov System

Xiaofei Zhao
Department of Mathematics, National University of Singapore, Singapore 119076, Singapore

Received 10 April 2014; accepted 26 May 2015
Published online 24 June 2015 in Wiley Online Library (wileyonlinelibrary.com).
DOI 10.1002/num.21994

In this article, we propose an exponential wave integrator sine pseudospectral (EWI-SP) method for solving the Klein–Gordon–Zakharov (KGZ) system. The numerical method is based on a Deuflhard-type exponential wave integrator for temporal integrations and the sine pseudospectral method for spatial discretizations. The scheme is fully explicit, time reversible and very efficient due to the fast algorithm. Rigorous finite time error estimates are established for the EWI-SP method in energy space with no CFL-type conditions which show that the method has second order accuracy in time and spectral accuracy in space. Extensive numerical experiments and comparisons are done to confirm the theoretical studies. Numerical results suggest the EWI-SP allows large time steps and mesh size in practical computing. Numer Methods Partial Differential Eq 32: 266–291, 2016

Keywords: error estimate; explicit scheme; exponential wave integrator; Klein–Gordon–Zakharov system; large time step; pseudospecral method

I. INTRODUCTION

The nondimensional Klein–Gordon–Zakharov (KGZ) system [1–4] in d-dimensions ($d = 1, 2, 3$) reads as the following,

$$\partial_{tt}\psi(\mathbf{x},t) - \Delta\psi(\mathbf{x},t) + \psi(\mathbf{x},t) + \psi(\mathbf{x},t)\phi(\mathbf{x},t) + \lambda|\psi|^2\psi(\mathbf{x},t) = 0, \tag{1.1a}$$

$$\partial_{tt}\phi(\mathbf{x},t) - \Delta\phi(\mathbf{x},t) - \Delta(|\psi(\mathbf{x},t)|^2) = 0, \qquad \mathbf{x} \in \mathbb{R}^d, \quad t > 0, \tag{1.1b}$$

with given initial conditions

$$\psi(\mathbf{x},0) = \psi^{(0)}(\mathbf{x}), \quad \partial_t\psi(\mathbf{x},0) = \psi^{(1)}(\mathbf{x}), \quad \phi(\mathbf{x},0) = \phi^{(0)}(\mathbf{x}), \quad \partial_t\phi(\mathbf{x},0) = \phi^{(1)}(\mathbf{x}). \tag{1.2}$$

Correspondence to: Xiaofei Zhao, Department of Mathematics, National University of Singapore, Singapore 119076 (e-mail: zhxfnus@gmail.com)
Contract grant sponsor: Ministry of Education of Singapore; contract grant number: R-146-000-196-112

Here, the unknowns $\psi = \psi(\mathbf{x}, t)$ and $\phi = \phi(\mathbf{x}, t)$ are two complex-valued scalar fields, $\mathbf{x}$ is the spatial variable, t is the temporal variable, and $\lambda \in \mathbb{R}$ is a given parameter. The above KGZ system can be derived from the two-fluid Euler–Maxwell system [5, 6] and is known as a classical model to describe the interactions between the Langmuir waves and ion acoustic waves in a plasma [7, 8], where ψ and ϕ are the fast time scale component of electric field raised by electrons and the derivation of ion density from its equilibrium, respectively. The cubic nonlinearity $\lambda|\psi|^2\psi$ in (1.1a) describes the nonlinear self-interactions of the electric field similarly as the Klein–Gordon equation [9], with $\lambda > 0$ for the defocusing case and $\lambda < 0$ for focusing case. Nonlinearities as higher order power laws, that is, $\lambda|\psi|^{2p}\psi$, $\Delta(|\psi|^{2q})$ for integers $p, q > 1$ are also considered in literature for generalizations [3, 4, 10].

Theoretically, the KGZ (1.1) has gained a lot of attentions in the literature. The well posedness of the KGZ have been studied and well established in [11–15, 39]. It is easy to see that the KGZ system (1.1) is time symmetric or time reversible, that is, changing $t \to -t$ in (1.1) the equations remain the same. The inheritance of time symmetry property in the discrete level of numerical methods is known as a key issue to provide good long-time performance of numerical approximations as illustrated in [16–18]. The KGZ system conserves the total *energy* [14, 15] when ϕ is real-valued, that is, for $t \geq 0$,

$$\begin{aligned} E(t) &:= \int_{\mathbb{R}^d} [|\partial_t\psi|^2 + |\nabla\psi|^2 + |\psi|^2 + \frac{1}{2}|\nabla\varphi|^2 + \frac{1}{2}|\phi|^2 + \phi \cdot |\psi|^2 + \frac{\lambda}{2}|\psi|^4] d\mathbf{x} \\ &\equiv E(0), \end{aligned} \tag{1.3}$$

where φ is defined via

$$\Delta\varphi = \partial_t\phi, \quad \text{with} \quad \lim_{|\mathbf{x}|\to\infty} \varphi = 0. \tag{1.4}$$

Solitary wave solutions (or solitons) [19] of the KGZ have also been pointed out in [3, 4]. Recent studies have been paid to the KGZ in some limit regimes [14, 15].

For numerical aspects of KGZ, the numerical methods proposed in the literature are limited. Wang et al. proposed some energy conservative finite difference time domain methods in [1] which conserves the energy (1.3) in a discrete level. Chen et al. later proposed a conservative finite difference scheme with a θ parameter. However, these methods are fully implicit and at each time step, a nonlinear problem has to be solved very accurately which is quite time-consuming. Explicit leap-frog finite difference methods are considered in [4], which naturally suffers from stability problems. Besides finite difference methods, some high order methods in spatial discretization are also considered. Ghoreishi et al. used Chebyshev cardinal functions in [20], and Dehghan et al. used the differential quadrature and globally radial basis functions in [3]. However, temporaly they only considered some first order finite difference approximations which together with the spatial discretizations will lead to some matrix computational problems without fast algorithms. Recently, Bao et al. [21] proposed an efficient and accurate three-level scheme for the KGZ based on a Gautschi-type [22] exponential wave integrator and the sine pseudospectral method (GISP). The exponential wave integrators (EWIs) are known to have many superior properties for integrating the wave type differential equations and are well illustrated in [16–18, 23, 40]. However, by borrowing the techniques to establish the error estimates for the Klein–Gordon equation with EWIs [9], the authors are constrained to obtain error bounds for the GISP under a CFL-type constraint. The constraint there is the stability condition to provide the finite time convergence, that is, the practical stability [24]. Asymptotically, the required CFL-type condition in [9] for the GISP is the same as the stability condition for the explicit Leap-frog finite difference scheme. The

CFL-type condition for finite time convergence of EWIs should not be essential from the classical studies in [16–18, 23, 40].

In this work, we consider an EWI based on the Deuflhard-type quadrature [25] for temporal approximations and sine pseudospectral method for spatial discretizations. The scheme can proceed in a two-level format, and is fully explicit, time reversible and very efficient due to the fast discrete sine transform. By working with the two-level scheme in the correct energy space, rigorous finite time error estimates for the proposed exponential wave integrator sine pseudospectral (EWI-SP) method are established without any CFL-type conditions. The results show that the method has the same accuracy order as the one proposed in [21], that is the second order accuracy in time and spectral accuracy in space. Numerical experiments are done to justify the theoretical results. Extensive numerical results suggest that the EWI-SP is very stable and allows use of large time steps and mesh size in practical computing, while the GISP method in [9] does suffer from a stability constraint. Comparisons between the two methods also show the EWI-SP has smaller approximation error under the same time step and mesh size. It is believed that the numerical method and proof technique can also be applied to the Zakharov equations [26] and the Klein–Gordon–Schrödinger equations [27].

The rest of the article is organized as follows. In Section II, we propose and analyze the EWI-SP method. In Section III, we give and prove the main error estimate results for the proposed EWI-SP. Numerical results and comparisons are reported in Section IV to confirm the theoretical studies. Some concluding remarks are given in Section V. Throughout this article, we adopt the notation $A \lesssim B$ to represent that there exists a generic constant $C > 0$, which is independent of the time step τ (or n) and mesh size h, such that $|A| \leq CB$.

II. AN EXPONENTIAL WAVE INTEGRATOR PSEUDOSPECTRAL METHOD

In this section, we shall propose the exponential wave integrator based on the Deulfhard-type quadrature and sine pseudospectral discretization for solving the KGZ (2.1). We shall first derive the scheme and then analyze some basic properties of the method. For simplicity of notations, we shall only present the numerical method and the analysis in one space dimension (1D). Generalizations to higher dimensions are straightforward with tensor products and results in this section remain valid with modifications to higher-order Sobolev spaces.

A. Numerical Scheme

Due to the fast decay of the solutions of KGZ at the far field [1, 2, 11–15], from numerical aspects, we truncate the whole space problem onto a finite interval $\Omega = (a, b)$ in 1D with zero boundary conditions, that is,

$$\partial_{tt}\psi(x,t) - \partial_{xx}\psi(x,t) + \psi(x,t) + \psi(x,t)\phi(x,t) + \lambda|\psi^2|\psi(x,t) = 0, \tag{2.1a}$$

$$\partial_{tt}\phi(x,t) - \partial_{xx}\phi(x,t) - \partial_{xx}(|\psi^2(x,t)|) = 0, \quad x \in \Omega, \quad t > 0, \tag{2.1b}$$

$$\psi(a,t) = \psi(b,t) = 0, \quad \phi(a,t) = \phi(b,t) = 0, \quad t \geq 0, \tag{2.1c}$$

$$\psi(x,0) = \psi^{(0)}(x), \quad \partial_t\psi(x,0) = \psi^{(1)}(x), \tag{2.1d}$$

$$\phi(x,0) = \phi^{(0)}(x), \quad \partial_t\phi(x,0) = \phi^{(1)}(x), \quad x \in \overline{\Omega} = [a,b]. \tag{2.1e}$$

Here, a and b are usually chosen sufficient large such that the truncation error at the boundary is negligible. We remark that one can consider the absorbing boundary conditions [28] or perfectly matched layer techniques [29] for further improvements. Choose the spatial mesh size $h = \Delta x = (b-a)/N$ for N an even positive integer, the time step size $\tau = \Delta t > 0$ and denote the grid points and the time steps by

$$x_j := a + jh, \quad t_n := n\tau, \quad j = 0, 1, \ldots N, \quad n = 0, 1, \ldots. \tag{2.2}$$

Define

$$X_N := \text{ span } \left\{ \phi_l(x) = \sin(\mu_l(x-a)) \ : \ x \in \overline{\Omega},\ \mu_l = \frac{\pi l}{b-a},\ l = 1, \ldots, N-1 \right\},$$
$$Y_N := \left\{ v = (v_0, v_1, \ldots, v_N) \in \mathbb{C}^{N+1} \ : \ v_0 = v_N = 0 \right\}.$$

For a general function $v(x)$ on $\overline{\Omega} = [a,b]$ and a vector $v \in Y_N$, let $P_N : L^2(\Omega) \to X_N$ be the standard L^2- projection operator onto X_N, $I_N : C(\Omega) \to X_N$ and $I_N : Y_N \to X_N$ be the trigonometric interpolation operator [30, 31], that is,

$$(P_N v)(x) = \sum_{l=1}^{N-1} \widehat{v}_l \sin(\mu_l(x-a)), \quad (I_N v)(x) = \sum_{l=1}^{N-1} \widetilde{v}_l \sin(\mu_l(x-a)), \quad a \le x \le b, \tag{2.3}$$

with

$$\widehat{v}_l = \frac{2}{b-a} \int_a^b v(x) \sin(\mu_l(x-a)) dx, \qquad \widetilde{v}_l = \frac{2}{N} \sum_{j=1}^{N-1} v_j \sin(\mu_l(x_j - a)), \tag{2.4}$$

where v_j is interpreted as $v(x_j)$. It is clear that P_N and I_N are identical operators over X_N. The sine spectral method [30, 31] for spatial discretizations of equations (2.1) becomes: find $\psi_N(x,t)$, $\phi_N(x,t) \in X_N$, such that

$$\partial_{tt}\psi_N(x,t) - \partial_{xx}\psi_N(x,t) + \psi_N(x,t) + \psi_N(x,t)\phi_N(x,t) + \lambda|\psi_N|^2\psi_N(x,t) = 0,$$
$$\partial_{tt}\phi_N(x,t) - \partial_{xx}\phi_N(x,t) - \partial_{xx}(|\psi_N(x,t)|^2) = 0, \quad x \in \Omega, \quad t > 0.$$

Due to the orthogonality of the sine basis functions [30, 31], we have for $l = 1, \ldots, N-1$ and $w \in \mathbb{R}$, when $t = t_n + w$ is near $t_n (n = 0, 1, \ldots)$,

$$\widehat{\psi}_l''(t_n + w) + \beta_l^2 \widehat{\psi}_l(t_n + w) + \widehat{(f_N)}_l^n(w) = 0, \tag{2.6a}$$

$$\widehat{\phi}_l''(t_n + w) + \mu_l^2 \widehat{\phi}_l(t_n + w) + \mu_l^2 \widehat{(g_N)}_l^n(w) = 0, \tag{2.6b}$$

where we define

$$f_N^n(x,w) := \psi_N \phi_N(x, t_n + w) + \lambda|\psi_N|^2 \psi_N(x, t_n + w), \quad g_N^n(x,w) := |\psi_N(x, t_n + w)|^2,$$

and

$$\beta_l := \sqrt{1 + \mu_l^2}, \qquad l = 1, \ldots, N-1. \tag{2.7}$$

The exponential wave integrator [16, 18, 22, 23, 25] begins with the variation-of-constant formula of the ODEs (2.6): for $l = 1, \dots, N-1$,

$$\widehat{\psi}_l(t_n + w) = \cos(\beta_l w)\widehat{\psi}_l(t_n) + \frac{\sin(\beta_l w)}{\beta_l}\widehat{\psi}'_l(t_n) - \int_0^w \frac{\sin(\beta_l(w-s))}{\beta_l}\widehat{(f_N)}^n_l(s)ds, \tag{2.8a}$$

$$\widehat{\phi}_l(t_n + w) = \cos(\mu_l w)\widehat{\phi}_l(t_n) + \frac{\sin(\mu_l w)}{\mu_l}\widehat{\phi}'_l(t_n) - \mu_l \int_0^w \sin(\mu_l(w-s))\widehat{(g_N)}^n_l(s)ds. \tag{2.8b}$$

Differentiating (2.8) with respect to w, we obtain

$$\begin{aligned}\widehat{\psi}'_l(t_n + w) &= -\beta_l \sin(\beta_l w)\widehat{\psi}_l(t_n) + \cos(\beta_l w)\widehat{\psi}'_l(t_n) \\ &\quad - \int_0^w \cos(\beta_l(w-s))\widehat{(f_N)}^n_l(s)ds, \end{aligned} \tag{2.9a}$$

$$\begin{aligned}\widehat{\phi}'_l(t_n + w) &= -\mu_l \sin(\mu_l w)\widehat{\phi}_l(t_n) + \cos(\mu_l w)\widehat{\phi}'_l(t_n) \\ &\quad - \mu_l^2 \int_0^w \cos(\mu_l(w-s))\widehat{(g_N)}^n_l(s)ds. \end{aligned} \tag{2.9b}$$

Applying the standard trapezoidal rule or the Deuflhard-type quadrature [25] to those unknown integrations in (2.8) and (2.9), and then set $w = \tau$, we get

$$\widehat{\psi}_l(t_{n+1}) \approx \cos(\beta_l \tau)\widehat{\psi}_l(t_n) + \frac{\sin(\beta_l \tau)}{\beta_l}\widehat{\psi}'_l(t_n) - \frac{\tau \sin(\beta_l \tau)}{2\beta_l}\widehat{(f_N)}^n_l(0), \tag{2.10a}$$

$$\widehat{\phi}_l(t_{n+1}) \approx \cos(\mu_l \tau)\widehat{\phi}_l(t_n) + \frac{\sin(\mu_l \tau)}{\mu_l}\widehat{\phi}'_l(t_n) - \frac{\tau \mu_l \sin(\mu_l \tau)}{2}\widehat{(g_N)}^n_l(0), \tag{2.10b}$$

$$\begin{aligned}\widehat{\psi}'_l(t_{n+1}) &\approx -\beta_l \sin(\beta_l \tau)\widehat{\psi}_l(t_n) + \cos(\beta_l \tau)\widehat{\psi}'_l(t_n) \\ &\quad - \frac{\tau}{2}\left[\cos(\beta_l \tau)\widehat{(f_N)}^n_l(0) + \widehat{(f_N)}^n_l(\tau)\right], \end{aligned} \tag{2.10c}$$

$$\begin{aligned}\widehat{\phi}'_l(t_{n+1}) &\approx -\mu_l \sin(\mu_l \tau)\widehat{\phi}_l(t_n) + \cos(\mu_l \tau)\widehat{\phi}'_l(t_n) \\ &\quad - \frac{\tau \mu_l^2}{2}\left[\cos(\mu_l \tau)\widehat{(g_N)}^n_l(0) + \widehat{(g_N)}^n_l(\tau)\right]. \end{aligned} \tag{2.10d}$$

The sine transform coefficients in (2.10) are given by the integration defined in (2.4) which is not suitable for practical computing, so by approximating the integral in (2.4) by a quadrature rule on the grids $\{x_j : j = 0, \dots, N\}$ [30, 31], we present the efficient pseudospectral implementation by using the interpolation stated in (2.4) rather than the projection (integration).

Thus, a detailed *exponential wave integrator sine pseudospectral* (EWI-SP) method reads as follows. Denote $\psi_j^n, \dot{\psi}_j^n$, ϕ_j^n and $\dot{\phi}_j^n (j = 0, \dots, N, n = 0, 1, \dots)$ be the approximations to $\psi(x_j, t_n)$, $\partial_t \psi(x_j, t_n)$, $\phi(x_j, t_n)$ and $\partial_t \phi(x_j, t_n)$, respectively. Choose $\psi_j^0 = \psi_j^{(0)}$, $\dot{\psi}_j^0 = \psi_j^{(1)}$, $\phi_j^0 = \phi_j^{(0)}$, $\dot{\phi}_j^0 = \phi_j^{(1)}$, then for $n = 0, 1, \dots$,

$$\psi_j^{n+1} = \sum_{l=1}^{N-1} \widetilde{\psi}_l^{n+1} \sin(\mu_l(x_j - a)), \quad \phi_j^{n+1} = \sum_{l=1}^{N-1} \widetilde{\phi}_l^{n+1} \sin(\mu_l(x_j - a)), \tag{2.11a}$$

$$\dot{\psi}_j^{n+1} = \sum_{l=1}^{N-1} \widetilde{(\dot{\psi})}_l^{n+1} \sin(\mu_l(x_j - a)), \quad \dot{\phi}_j^{n+1} = \sum_{l=1}^{N-1} \widetilde{(\dot{\phi})}_l^{n+1} \sin(\mu_l(x_j - a)), \tag{2.11b}$$

where

$$\widetilde{\psi}_l^{n+1} = \cos(\beta_l\tau)\widetilde{\psi}_l^n + \frac{\sin(\beta_l\tau)}{\beta_l}\widetilde{(\dot{\psi})}_l^n - \frac{\tau\sin(\beta_l\tau)}{2\beta_l}\widetilde{f}_l^n, \tag{2.12a}$$

$$\widetilde{\phi}_l^{n+1} = \cos(\mu_l\tau)\widetilde{\phi}_l^n + \frac{\sin(\mu_l\tau)}{\mu_l}\widetilde{(\dot{\phi})}_l^n - \frac{\tau\mu_l\sin(\mu_l\tau)}{2}\widetilde{g}_l^n, \tag{2.12b}$$

$$\widetilde{(\dot{\psi})}_l^{n+1} = -\beta_l\sin(\beta_l\tau)\widetilde{\psi}_l^n + \cos(\beta_l\tau)\widetilde{(\dot{\psi})}_l^n - \frac{\tau}{2}\left[\cos(\beta_l\tau)\widetilde{f}_l^n + \widetilde{f}_l^{n+1}\right], \tag{2.12c}$$

$$\widetilde{(\dot{\phi})}_l^{n+1} = -\mu_l\sin(\mu_l\tau)\widetilde{\phi}_l^n + \cos(\mu_l\tau)\widetilde{(\dot{\phi})}_l^n - \frac{\tau\mu_l^2}{2}\left[\cos(\mu_l\tau)\widetilde{g}_l^n + \widetilde{g}_l^{n+1}\right], \tag{2.12d}$$

with

$$\widetilde{\psi}_l^n = \frac{2}{N}\sum_{j=0}^{N-1}\psi_j^n\sin(\mu_l(x_j-a)), \quad \widetilde{(\dot{\psi})}_l^n = \frac{2}{N}\sum_{j=0}^{N-1}\dot{\psi}_j^n\sin(\mu_l(x_j-a)), \tag{2.13a}$$

$$\widetilde{\phi}_l^n = \frac{2}{N}\sum_{j=0}^{N-1}\phi_j^n\sin(\mu_l(x_j-a)), \quad \widetilde{(\dot{\phi})}_l^n = \frac{2}{N}\sum_{j=0}^{N-1}\dot{\phi}_j^n\sin(\mu_l(x_j-a)), \tag{2.13b}$$

$$\widetilde{f}_l^n = \frac{2}{N}\sum_{j=0}^{N-1}(\psi_j^n\phi_j^n + \lambda|\psi_j^n|^2\psi_j^n)\sin(\mu_l(x_j-a)), \tag{2.13c}$$

$$\widetilde{g}_l^n = \frac{2}{N}\sum_{j=0}^{N-1}|\psi_j^n|^2\sin(\mu_l(x_j-a)). \tag{2.13d}$$

Remark 2.1. We remark here the zero Dirichlet boundary conditions could be replaced by homogenous Neumann or periodic boundary conditions, and when this is done the corresponding exponential time integrator cosine or Fourier pseudospectral method can be designed by simply changing the discrete sine transform used above into the discrete cosine or Fourier transform.

B. Properties and Analysis

The above EWI-SP method (2.11)–(2.13) is clearly fully explicit. It is easy to implement and very efficient due to the fast discrete sine transform. The memory cost is $O(N)$ and the computational cost per time step is $O(N\log N)$. Moreover, the scheme is time reversible due to the following equivalent form.

Proposition 2.1. (Time reversible) *For the proposed EWI-SP method (2.11)–(2.13), the step (2.12) in the scheme can be reformulated into following the three-step formalism for $n \geq 1$,*

$$\widetilde{\psi}_l^{n+1} + \widetilde{\psi}_l^{n-1} = 2\cos(\beta_l\tau)\widetilde{\psi}_l^n - \frac{\tau\sin(\beta_l\tau)}{\beta_l}\widetilde{f}_l^n, \quad l = 1,\ldots,N-1, \tag{2.14a}$$

$$\widetilde{\phi}_l^{n+1} + \widetilde{\phi}_l^{n-1} = 2\cos(\mu_l\tau)\widetilde{\phi}_l^n - \tau\mu_l\sin(\mu_l\tau)\widetilde{g}_l^n, \tag{2.14b}$$

$$\widetilde{(\dot{\psi})}_l^{n+1} + \widetilde{(\dot{\psi})}_l^{n-1} = 2\cos(\beta_l\tau)\widetilde{(\dot{\psi})}_l^n - \frac{\tau}{2}(\widetilde{f}_l^{n+1} - \widetilde{f}_l^{n-1}), \tag{2.14c}$$

$$\widetilde{(\dot{\phi})}_l^{n+1} + \widetilde{(\dot{\phi})}_l^{n-1} = 2\cos(\mu_l\tau)\widetilde{(\dot{\phi})}_l^{n} - \frac{\tau\mu_l^2}{2}(\widetilde{g}_l^{n+1} - \widetilde{g}_l^{n-1}). \tag{2.14d}$$

Consequently, the EWI-SP method is time reversible, that is, exchanging $n+1 \leftrightarrow n-1$ and $\tau \leftrightarrow -\tau$, the scheme remains the same.

Proof. For $n \geq 1$, switching $n \to n-1$ in (2.12c) and then substituting it into (2.12a), we get

$$\widetilde{\psi}_l^{n+1} = \cos(\beta_l\tau)\widetilde{\psi}_l^{n} - \sin^2(\beta_l\tau)\widetilde{\psi}_l^{n-1} + \frac{\sin(\beta_l\tau)\cos(\beta_l\tau)}{\beta_l}\widetilde{(\dot{\psi})}_l^{n-1} - \frac{\tau\sin(\beta_l\tau)\cos(\beta_l\tau)}{2\beta_l}\widetilde{f}_l^{n-1} - \frac{\tau\sin(\beta_l\tau)}{\beta_l}\widetilde{f}_l^{n}. \tag{2.15}$$

Switching $n \to n-1$ in (2.12a) and then multiplying on both sides by $\cos(\beta_l\tau)$, we get

$$\cos(\beta_l\tau)\widetilde{\psi}_l^{n} = \cos^2(\beta_l\tau)\widetilde{\psi}_l^{n-1} + \frac{\sin(\beta_l\tau)\cos(\beta_l\tau)}{\beta_l}\widetilde{(\dot{\psi})}_l^{n-1} - \frac{\tau\sin(\beta_l\tau)\cos(\beta_l\tau)}{2\beta_l}\widetilde{f}_l^{n-1}. \tag{2.16}$$

Subtracting (2.16) from (2.15), we obtain (2.14a) and similarly, we can obtain (2.14b). Switching $n \to n-1$ in (2.12a) and then substituting it into (2.12c), we obtain

$$\widetilde{(\dot{\psi})}_l^{n+1} = -\beta_l\sin(\beta_l\tau)\cos(\beta_l\tau)\widetilde{\psi}_l^{n-1} - \sin^2(\beta_l\tau)\widetilde{(\dot{\psi})}_l^{n-1} + \frac{\tau\sin^2(\beta_l\tau)}{2}\widetilde{f}_l^{n-1} + \cos(\beta_l\tau)\widetilde{(\dot{\psi})}_l^{n} - \frac{\tau}{2}\left[\cos(\beta_l\tau)\widetilde{f}_l^{n} + \widetilde{f}_l^{n+1}\right]. \tag{2.17}$$

Switching $n \to n-1$ in (2.12c) and then multiplying on both sides by $\cos(\beta_l\tau)$, we obtain

$$\cos(\beta_l\tau)\widetilde{(\dot{\psi})}_l^{n} = -\beta_l\sin(\beta_l\tau)\cos(\beta_l\tau)\widetilde{\psi}_l^{n-1} + \cos^2(\beta_l\tau)\widetilde{(\dot{\psi})}_l^{n-1} - \frac{\tau\cos(\beta_l\tau)}{2}\left[\cos(\beta_l\tau)\widetilde{f}_l^{n-1} + \widetilde{f}_l^{n}\right]. \tag{2.18}$$

Subtracting (2.18) from (2.17), we obtain (2.14b) and similarly, we can obtain (2.14d). Based on (2.14), interchanging $n+1 \leftrightarrow n-1$ and $\tau \leftrightarrow -\tau$, the scheme remains the same. Thus, the proposed EWI-SP method is time reversible. ■

Remark 2.2. In fact the three-step formalism of EWI-SP (2.14) is equivalent to (2.12), by choosing the starting values, that is, ψ^1, ϕ^1, $\dot{\psi}^1$, and $\dot{\phi}^1$, same as (2.12). The reverse direction of this fact can be proved by using mathematical induction on time grids index n. We omit the detailed proof here for brevity.

Remark 2.3. We remark that by means of the formalism (2.15) and (2.16), one can eliminate the time derivatives, that is, $\dot{\psi}^n$ and $\dot{\phi}^n$, in the EWI-SP if they are not of interests.

Thus, we can write down the scheme of EWI-SP (2.11)–(2.13) in the following three-level manner. Adopt the same notations as before and choose starting values $\psi_j^0 = \psi_j^{(0)}, \dot{\psi}_j^0 = \psi_j^{(1)}$, $\phi_j^0 = \phi_j^{(0)}, \dot{\phi}_j^0 = \phi_j^{(1)}$ and

$$\widetilde{\psi}_l^{1} = \cos(\beta_l\tau)\widetilde{\psi}_l^{0} + \frac{\sin(\beta_l\tau)}{\beta_l}\widetilde{(\dot{\psi})}_l^{0} - \frac{\tau\sin(\beta_l\tau)}{2\beta_l}\widetilde{f}_l^{0},$$

$$
\begin{aligned}
\widetilde{\phi}_l^1 &= \cos(\mu_l\tau)\widetilde{\phi}_l^0 + \frac{\sin(\mu_l\tau)}{\mu_l}\widetilde{(\dot{\phi})}_l^0 - \frac{\tau\mu_l\sin(\mu_l\tau)}{2}\widetilde{g}_l^0,\\
\widetilde{(\dot{\psi})}_l^1 &= -\beta_l\sin(\beta_l\tau)\widetilde{\psi}_l^0 + \cos(\beta_l\tau)\widetilde{(\dot{\psi})}_l^0 - \frac{\tau}{2}\left[\cos(\beta_l\tau)\widetilde{f}_l^0 + \widetilde{f}_l^1\right],\\
\widetilde{(\dot{\phi})}_l^1 &= -\mu_l\sin(\mu_l\tau)\widetilde{\phi}_l^0 + \cos(\mu_l\tau)\widetilde{(\dot{\phi})}_l^0 - \frac{\tau\mu_l^2}{2}\left[\cos(\mu_l\tau)\widetilde{g}_l^0 + \widetilde{g}_l^1\right],
\end{aligned}
$$

then for $n \geq 1$,

$$
\begin{aligned}
&\widetilde{\psi}_l^{n+1} + \widetilde{\psi}_l^{n-1} = 2\cos(\beta_l\tau)\widetilde{\psi}_l^n - \frac{\tau\sin(\beta_l\tau)}{\beta_l}\widetilde{f}_l^n,\\
&\widetilde{\phi}_l^{n+1} + \widetilde{\phi}_l^{n-1} = 2\cos(\mu_l\tau)\widetilde{\phi}_l^n - \tau\mu_l\sin(\mu_l\tau)\widetilde{g}_l^n,\\
&\widetilde{(\dot{\psi})}_l^{n+1} + \widetilde{(\dot{\psi})}_l^{n-1} = 2\cos(\beta_l\tau)\widetilde{(\dot{\psi})}_l^n - \frac{\tau}{2}(\widetilde{f}_l^{n+1} - \widetilde{f}_l^{n-1}),\\
&\widetilde{(\dot{\phi})}_l^{n+1} + \widetilde{(\dot{\phi})}_l^{n-1} = 2\cos(\mu_l\tau)\widetilde{(\dot{\phi})}_l^n - \frac{\tau\mu_l^2}{2}(\widetilde{g}_l^{n+1} - \widetilde{g}_l^{n-1}), \quad l = 1, \ldots, N-1,
\end{aligned}
$$

with $\widetilde{f}_l^n$ and $\widetilde{g}_l^n$ defined same as (2.13).

The Deuflhard-type EWI is also known equivalent to a time-splitting method for temporal approximations [17, 32] of time-dependent systems, so the proposed EWI-SP (2.11)–(2.13) can be derived from a time-splitting pseudospectral discretization approach. In fact, denote $u := \partial_t\psi$, $v := \partial_t\phi$, then rewrite the KGZ system into a first-order system and split it into

$$
\mathcal{A}: \partial_t\begin{pmatrix}\psi\\ u\\ \phi\\ v\end{pmatrix} = \begin{pmatrix}0\\ -\psi\phi - \lambda|\psi|^2\psi\\ 0\\ \Delta(|\psi|^2)\end{pmatrix}, \quad \mathcal{B}: \partial_t\begin{pmatrix}\psi\\ u\\ \phi\\ v\end{pmatrix} = \begin{pmatrix}u\\ \Delta\psi - \psi\\ v\\ \Delta\phi\end{pmatrix}.
$$

The system $\mathcal{A}$ can be solved exactly, and by spectral method system $\mathcal{B}$ can also be integrated exactly in phase space. Then by using the second order Strang composition as $e^{\mathcal{A}\frac{\tau}{2}}e^{\mathcal{B}\tau}e^{\mathcal{A}\frac{\tau}{2}}$, one can find the resulting numerical method is exactly same as the EWI-SP method (2.11)–(2.13). We refer the readers to [32] for more details about this topic.

Remark 2.4. Here, the reason why we choose not to derive the EWI-SP method directly from the splitting approach is because the error estimate of time-splitting method is very difficult. The establishment of rigorous error bounds of time-splitting method usually requires very complicate mathematical concepts and tools [33, 34]. However with the EWI approach, as shall be done in the next section, the error estimate can be obtained much more easily by means of the classical energy method.

C. Benchmark for Comparisons

As a benchmark for comparisons, we write down the Gautschi type exponential wave integrator sine pseudospectral method (shorted as GISP) proposed in [21]. The scheme of the GISP is given in the three level format as: choose initial values same as before and define $\psi^{n+1}, \phi^{n+1}, \dot{\psi}^{n+1}, \dot{\phi}^{n+1}$ for $n \geq 0$ as (2.11), then for $n = 0$,

$$\begin{cases} \widetilde{\psi}_l^1 = \cos(\beta_l\tau)\,\widetilde{\psi}_l^0 + \dfrac{\sin(\beta_l\tau)}{\beta_l}\widetilde{(\dot{\psi})}_l^0 + \dfrac{\cos(\beta_l\tau)-1}{\beta_l^2}\widetilde{f}_l^0, \\ \widetilde{\phi}_l^1 = \cos(\mu_l\tau)\,\widetilde{\phi}_l^0 + \dfrac{\sin(\mu_l\tau)}{\mu_l}\widetilde{(\dot{\phi})}_l^0 + [\cos(\mu_l\tau)-1]\,\widetilde{g}_l^0, \\ \widetilde{(\dot{\psi})}_l^1 = -\beta_l\sin(\beta_l\tau)\,\widetilde{\psi}_l^0 + \cos(\beta_l\tau)\,\widetilde{(\dot{\psi})}_l^0 - \dfrac{\sin(\beta_l\tau)}{\beta_l}\widetilde{f}_l^0, \\ \widetilde{(\dot{\phi})}_l^1 = -\mu_l\sin(\mu_l\tau)\,\widetilde{\phi}_l^0 + \cos(\mu_l\tau)\,\widetilde{(\dot{\phi})}_l^0 - \mu_l\sin(\mu_l\tau)\,\widetilde{g}_l^0, \end{cases} \tag{2.19}$$

and for $n \geq 1$,

$$\begin{cases} \widetilde{\psi}_l^{n+1} = -\widetilde{\psi}_l^{n-1} + 2\cos(\beta_l\tau)\,\widetilde{\psi}_l^n + \dfrac{2[\cos(\beta_l\tau)-1]}{\beta_l^2}\widetilde{f}_l^n, \\ \widetilde{\phi}_l^{n+1} = -\widetilde{\phi}_l^{n-1} + 2\cos(\mu_l\tau)\,\widetilde{\phi}_l^n + 2[\cos(\mu_l\tau)-1]\,\widetilde{g}_l^n, \\ \widetilde{(\dot{\psi})}_l^{n+1} = \widetilde{(\dot{\psi})}_l^{n-1} - 2\beta_l\sin(\beta_l\tau)\,\widetilde{\psi}_l^n - \dfrac{2\sin(\beta_l\tau)}{\beta_l}\widetilde{f}_l^n, \\ \widetilde{(\dot{\phi})}_l^{n+1} = \widetilde{(\dot{\phi})}_l^{n-1} - 2\mu_l\sin(\mu_l\tau)\,\widetilde{\phi}_l^n - 2\mu_l\sin(\mu_l\tau)\,\widetilde{g}_l^n. \end{cases} \tag{2.20}$$

The above GISP is also explicit, symmetric and the computational cost is the same as the EWI-SP method (2.11)–(2.13). However, the finite time error estimate of the GISP method given in [21] suffers a CFL-type condition $\tau \lesssim h$.

III. CONVERGENCE ANALYSIS

In this section, we shall establish the rigorous error estimate results of the EWI-SP (2.11)–(2.13) for solving the KGZ system (2.1), where the CFL-type condition required in [21] is removed. We shall first give the main theorem on the error bounds in the energy space $H^1 \times L^2$ for the variables ψ and ϕ, respectively, then prove the theorem by posterior error estimate techniques.

A. Main Theorem on Error Bounds in Energy Space

To state the main results, we introduce the subspace

$$H_s^m(\Omega) = \left\{ v \in H^m(\Omega) : \partial_x^{2k} v(a) = \partial_x^{2k} v(b) = 0,\ k \in \mathbb{N},\ 0 \leq 2k < m \right\} \in H^m \cap H_0^1,$$

for integer $m \geq 1$. To obtain the optimal error estimate results, we consider the sufficiently smooth and localized initial data for the KGZ system (2.1), and motivated from the analytical results for the KGZ equation in [11–15], we make the following assumptions: let $0 < T \leq T^*$ with T^* the maximum existence time of the solution $\psi(x,t)$ and $\phi(x,t)$ to problem (2.1); assume that for some integer $m_0 \geq 1$,

$$\psi \in C([0,T]; W^{1,\infty} \cap H_s^{m_0+1}) \cap C^1([0,T]; W^{1,4} \cap H_s^{m_0}) \cap C^2([0,T]; H^1),$$

$$\phi \in C([0,T]; L^\infty \cap H_s^{m_0+1}) \cap C^1([0,T]; L^4 \cap H_s^{m_0}) \cap C^2([0,T]; L^2). \tag{A}$$

Under assumption (A), for the function $\varphi(x,t)$ defined in (1.4), we should have

$$\varphi \in C([0,T]; H_s^{m_0+2}), \tag{3.1}$$

and then we let

$$K_1 := \max\left\{||\psi||_{L^\infty([0,T];L^\infty\cap H^2)}, ||\partial_t\psi||_{L^\infty([0,T];H^1)}\right\},$$

$$K_2 := \max\left\{||\phi||_{L^\infty([0,T];L^\infty\cap H^1)}, ||\partial_x\varphi||_{L^\infty([0,T];L^2)}\right\}.$$

Denote the trigonometric interpolations of numerical solutions as

$$\psi_I^n(x) := I_N(\psi^n)(x), \quad \phi_I^n(x) := I_N(\phi^n)(x), \quad \dot{\psi}_I^n(x) := I_N(\dot{\psi}^n)(x), \quad x \in \Omega, \tag{3.2}$$

and an auxiliary function instead of $\dot{\phi}^n$ as

$$\rho_I^n(x) = \sum_{l=1}^{N-1} \widetilde{\rho}_l^n \sin(\mu_l(x-a)), \quad \text{with} \quad \widetilde{\rho}_l^n := \frac{1}{\mu_l}\widetilde{(\dot{\phi})}_l^n. \tag{3.3}$$

Define the "error" functions as

$$e_\psi^n(x) := \psi(x,t_n) - \psi_I^n(x), \quad e_\phi^n(x) := \phi(x,t_n) - \phi_I^n(x), \quad n = 0,1\ldots, \tag{3.4a}$$

$$\dot{e}_\psi^n(x) := \partial_t\psi(x,t_n) - \dot{\psi}_I^n(x), \quad e_\rho^n(x) := \partial_x\varphi(x,t_n) - \rho_I^n(x), \quad x \in \Omega, \tag{3.4b}$$

where the function $\varphi(x,t)$ is given in (1.4), then we have the following main error estimate result:

Theorem 3.1. *Let ψ^n, ϕ^n, $\dot{\psi}^n$ and $\dot{\phi}^n$ be the numerical approximations obtained from the EWI-SP method (2.11)–(2.13). Under the assumption (A), there exist two constants τ_0, $h_0 > 0$, independent of τ (or n) and h, such that for any $0 < \tau < \tau_0$, $0 < h < h_0$,*

$$||\dot{e}_\psi^n||_{L^2} + ||e_\psi^n||_{H^1} + ||e_\rho^n||_{L^2} + ||e_\phi^n||_{L^2} \lesssim \tau^2 + h^{m_0}, \quad n = 0,1,\ldots,\frac{T}{\tau}, \tag{3.5a}$$

$$||\psi_I^n||_{H^1} \le K_1 + 1, \qquad ||\phi_I^n||_{L^2} \le K_2 + 1, \qquad ||\psi^n||_{l^\infty} \le K_1 + 1, \tag{3.5b}$$

$$||\dot{\psi}_I^n||_{L^2} \le K_1 + 1, \qquad ||\rho_I^n||_{L^2} \le K_2 + 1. \tag{3.5c}$$

B. Proof of the Main Theorem

To proceed to the proof, we introduce the following notations. Let ψ, ϕ be the exact solution of the KGZ system (2.1). Denote the L^2-projected solution as

$$\psi_N(x,t) := P_N(\psi(x,t)) = \sum_{l=1}^{N-1} \widehat{\psi}_l(t)\sin(\mu_l(x-a)),$$

$$\phi_N(x,t) := P_N(\phi(x,t)) = \sum_{l=1}^{N-1} \widehat{\phi}_l(t)\sin(\mu_l(x-a)), \qquad x \in \Omega,\ t \ge 0, \tag{3.6}$$

and the projected error functions as

$$e^n_{\psi,N}(x) := P_N(e^n_\psi(x)), \quad e^n_{\phi,N}(x) := P_N(e^n_\phi(x)),$$
$$\dot{e}^n_{\psi,N}(x) := P_N(e^n_{\dot\psi}(x)), \quad e^n_{\rho,N}(x) := P_N(e^n_\rho(x)), \qquad n = 0, 1, \ldots, \frac{T}{\tau}, \tag{3.7}$$

where from (3.4) and noticing (1.4), the corresponding coefficients in the frequency space should satisfy

$$\widehat{(e_\psi)}^n_l = \widehat{\psi}_l(t_n) - \widetilde{\psi}^n_l, \qquad \widehat{(e_\phi)}^n_l = \widehat{\phi}_l(t_n) - \widetilde{\phi}^n_l, \qquad l = 1, \ldots, N-1,$$
$$\widehat{(\dot{e}_\psi)}^n_l = \widehat{\psi}'_l(t_n) - \widetilde{(\dot\psi)}^n_l, \qquad \widehat{(e_\rho)}^n_l = \frac{1}{\mu_l}\widehat{\phi}'_l(t_n) - \widetilde{\rho}^n_l, \qquad n = 0, 1, \ldots, \frac{T}{\tau}. \tag{3.8}$$

Based on (2.10), define the local truncation errors for $n = 0, 1, \ldots, \frac{T}{\tau} - 1$ as

$$\xi^n_\psi(x) := \sum_{l=1}^{N-1} \widehat{(\xi_\psi)}^n_l \sin(\mu_l(x_j - a)), \quad \xi^n_\phi(x) := \sum_{l=1}^{N-1} \widehat{(\xi_\phi)}^n_l \sin(\mu_l(x_j - a)),$$
$$\dot\xi^n_\psi(x) := \sum_{l=1}^{N-1} \widehat{(\dot\xi_\psi)}^n_l \sin(\mu_l(x_j - a)), \quad \xi^n_\rho(x) := \sum_{l=1}^{N-1} \widehat{(\xi_\rho)}^n_l \sin(\mu_l(x_j - a)), \quad x \in \Omega,$$

where

$$\widehat{(\xi_\psi)}^n_l = \widehat{\psi}_l(t_{n+1}) - \cos(\beta_l\tau)\,\widehat{\psi}_l(t_n) - \frac{\sin(\beta_l\tau)}{\beta_l}\widehat{\psi}'_l(t_n) + \frac{\tau\sin(\beta_l\tau)}{2\beta_l}\widehat{f}^n_l(0), \tag{3.9a}$$

$$\widehat{(\xi_\phi)}^n_l = \widehat{\phi}_l(t_{n+1}) - \cos(\mu_l\tau)\,\widehat{\phi}_l(t_n) - \frac{\sin(\mu_l\tau)}{\mu_l}\widehat{\phi}'_l(t_n) + \frac{\tau\mu_l\sin(\mu_l\tau)}{2}\widehat{g}^n_l(0), \tag{3.9b}$$

$$\widehat{(\dot\xi_\psi)}^n_l = \widehat{\psi}'_l(t_{n+1}) + \beta_l\sin(\beta_l\tau)\widehat{\psi}_l(t_n) - \cos(\beta_l\tau)\widehat{\psi}'_l(t_n) + \frac{\tau}{2}[\cos(\beta_l\tau)\widehat{f}^n_l(0) + \widehat{f}^n_l(\tau)], \tag{3.9c}$$

$$\widehat{(\xi_\rho)}^n_l = \frac{1}{\mu_l}\widehat{\phi}'_l(t_{n+1}) + \sin(\mu_l\tau)\widehat{\phi}_l(t_n) - \frac{\cos(\mu_l\tau)}{\mu_l}\widehat{\phi}'_l(t_n) + \frac{\tau\mu_l}{2}[\cos(\mu_l\tau)\widehat{g}^n_l(0) + \widehat{g}^n_l(\tau)], \tag{3.9d}$$

with

$$f^n(x,s) := \psi\phi(x, t_n + s) + \lambda|\psi|^2\psi(x, t_n + s), \quad g^n(x,s) := |\psi(x, t_n + s)|^2. \tag{3.10}$$

Adding the local truncation errors (3.9) from the scheme (2.12) and noting (3.3), we are led to the error equations for $n = 0, 1, \ldots, \frac{T}{\tau} - 1$ and $l = 1, \ldots, N-1$,

$$\widehat{(e_\psi)}^{n+1}_l = \cos(\beta_l\tau)\,\widehat{(e_\psi)}^n_l + \frac{\sin(\beta_l\tau)}{\beta_l}\widehat{(\dot{e}_\psi)}^n_l + \widehat{(\xi_\psi)}^n_l - \widehat{(\eta_\psi)}^n_l, \tag{3.11a}$$

$$\widehat{(e_\phi)}^{n+1}_l = \cos(\mu_l\tau)\,\widehat{(e_\phi)}^n_l + \frac{\sin(\mu_l\tau)}{\mu_l}\widehat{(e_\rho)}^n_l + \widehat{(\xi_\phi)}^n_l - \widehat{(\eta_\phi)}^n_l, \tag{3.11b}$$

$$\widehat{(\dot{e}_\psi)}_l^{n+1} = -\beta_l \sin(\beta_l \tau)\,\widehat{(e_\psi)}_l^n + \cos(\beta_l \tau)\,\widehat{(\dot{e}_\psi)}_l^n + \widehat{(\dot{\xi}_\psi)}_l^n - \widehat{(\dot{\eta}_\psi)}_l^n, \tag{3.11c}$$

$$\widehat{(e_\rho)}_l^{n+1} = -\sin(\mu_l \tau)\,\widehat{(e_\phi)}_l^n + \frac{\cos(\mu_l \tau)}{\mu_l}\widehat{(e_\rho)}_l^n + \widehat{(\xi_\rho)}_l^n - \widehat{(\eta_\rho)}_l^n, \tag{3.11d}$$

where

$$\widehat{(\eta_\psi)}_l^n = \frac{\tau \sin(\beta_l \tau)}{2\beta_l}\left(\widehat{f}_l^n(0) - \widetilde{f}_l^n\right), \quad \widehat{(\eta_\phi)}_l^n = \frac{\tau \mu_l \sin(\mu_l \tau)}{2}\left(\widehat{g}_l^n(0) - \widetilde{g}_l^n\right), \tag{3.12a}$$

$$\widehat{(\dot{\eta}_\psi)}_l^n = \frac{\tau}{2}\left[\cos(\beta_l \tau)\left(\widehat{f}_l^n(0) - \widetilde{f}_l^n\right) + \widehat{f}_l^n(\tau) - \widetilde{f}_l^{n+1}\right], \tag{3.12b}$$

$$\widehat{(\eta_\rho)}_l^n = \frac{\tau \mu_l}{2}\left[\cos(\mu_l \tau)\left(\widehat{g}_l^n(0) - \widetilde{g}_l^n\right) + \widehat{g}_l^n(\tau) - \widetilde{g}_l^{n+1}\right], \tag{3.12c}$$

with the nonlinear error functions defined as

$$\eta_\psi^n(x) := \sum_{l=1}^{N-1} \widehat{(\eta_\psi)}_l^n \sin(\mu_l(x_j - a)), \quad \eta_\phi^n(x) := \sum_{l=1}^{N-1} \widehat{(\eta_\phi)}_l^n \sin(\mu_l(x_j - a)),$$

$$\dot{\eta}_\psi^n(x) := \sum_{l=1}^{N-1} \widehat{(\dot{\eta}_\psi)}_l^n \sin(\mu_l(x_j - a)), \quad \eta_\rho^n(x) := \sum_{l=1}^{N-1} \widehat{(\eta_\rho)}_l^n \sin(\mu_l(x_j - a)), \quad x \in \Omega.$$

Define the error energy functional as

$$\mathcal{E}(P, Q, R, S) := ||P||_{L^2}^2 + ||Q||_{H^1}^2 + ||R||_{L^2}^2 + ||S||_{L^2}^2, \tag{3.13}$$

for some arbitrary functions $P(x)$, $Q(x)$, $R(x)$ and $S(x)$ on Ω.

To prove Theorem 3.1, we establish the following lemmas. First of all, we review some important inequalities for the projection and interpolation defined in (2.3). Define the discrete H^1-norm as

$$||v||_{h^1} := \sqrt{||v||_{l^2}^2 + ||\delta_x^+ v||_{l^2}^2},$$

where

$$||v||_{l^2}^2 = h \sum_{j=1}^{N-1} |v_j|^2, \quad ||\delta_x^+ v||_{l^2}^2 = h \sum_{j=0}^{N-1} |\delta_x^+ v_j|^2,$$

for some $v \in Y_N$. Then we have

Lemma 3.2. *For any $v(x) \in H_s^m(\Omega)$ with $m \geq 1$, if $||\phi||_{H^m} \lesssim 1$, then we have estimates for the projection and interpolation as*

$$\|v - P_N v\|_{H^k} \lesssim h^{m-k}, \quad \|v - I_N v\|_{H^k} \lesssim h^{m-k}, \qquad 0 \leq k \leq m. \tag{3.14}$$

Moreover, if $v \in X_N \subset H_s^m$, then we have the equivalence of norms as

$$||v||_{h^1} \lesssim ||v||_{H^1} \lesssim ||v||_{h^1}. \tag{3.15}$$

Proof. Estimates (3.14) are standard results for spectral methods in [31]. For the second assertion, by directly computing and Paserval's identity we have

$$||\partial_x v||_{L^2}^2 = \frac{b-a}{2}\sum_{l=1}^{N-1}|\mu_l|^2|\widehat{v}_l|^2, \quad ||\delta_x^+ v||_{l^2}^2 = \frac{b-a}{2}\sum_{l=0}^{N-1}\frac{4}{h^2}\sin^2\left(\frac{\mu_l h}{2}\right)|\widehat{\phi}_l|^2.$$

Noting that now $|\mu_l| \lesssim |\frac{2}{h}\sin(\mu_l h/2)| \lesssim |\mu_l|$ for all $l = 1,\ldots,N-1$, we get the assertion (3.15). ∎

For the local truncation errors (3.9), we have estimates stated in the following lemma.

Lemma 3.3. *Based on the assumption (A), we have estimates for the local truncation errors as*

$$\mathcal{E}\left(\dot{\xi}_\psi^n, \xi_\psi^n, \xi_\rho^n, \xi_\phi^n\right) \lesssim \tau^6, \qquad n = 0, 1, \ldots, \frac{T}{\tau} - 1. \tag{3.16}$$

Proof. Applying the L^2-projection on both sides of (2.1), due to the orthogonality of basis functions and the variation-of-constant formula, the sine transform coefficients $\widehat{\psi_l}(t_n)$ and $\widehat{\phi_l}(t_n)$ should satisfy

$$\begin{cases} \widehat{\psi_l}(t_{n+1}) = \cos(\beta_l\tau)\,\widehat{\psi_l}(t_n) + \dfrac{\sin(\beta_l\tau)}{\beta_l}\widehat{\psi_l'}(t_n) - \displaystyle\int_0^\tau \frac{\sin(\beta_l(\tau-s))}{\beta_l}\widehat{f_l^n}(s)ds, \\ \widehat{\phi_l}(t_{n+1}) = \cos(\mu_l\tau)\,\widehat{\phi_l}(t_n) + \dfrac{\sin(\mu_l\tau)}{\mu_l}\widehat{\phi_l'}(t_n) - \mu_l\displaystyle\int_0^\tau \sin(\mu_l(\tau-s))\,\widehat{g_l^n}(s)ds, \\ \widehat{\psi_l'}(t_{n+1}) = -\beta_l\sin(\beta_l\tau)\,\widehat{\psi_l}(t_n) + \cos(\beta_l\tau)\,\widehat{\psi_l'}(t_n) - \displaystyle\int_0^\tau \cos(\beta_l(\tau-s))\,\widehat{f_l^n}(s)ds, \\ \dfrac{\widehat{\phi_l'}(t_{n+1})}{\mu_l} = -\sin(\mu_l\tau)\,\widehat{\phi_l}(t_n) + \dfrac{\cos(\mu_l\tau)}{\mu_l}\widehat{\phi_l'}(t_n) - \mu_l\displaystyle\int_0^\tau \cos(\mu_l(\tau-s))\,\widehat{g_l^n}(s)ds. \end{cases} \tag{3.17}$$

Adding (3.9) from (3.17), we get

$$\begin{aligned} \widehat{(\xi_\psi)}_l^n &= \int_0^\tau \frac{\sin(\beta_l(\tau-s))}{\beta_l}\widehat{f_l^n}(s)ds - \frac{\tau\sin(\beta_l\tau)}{2\beta_l}\widehat{f_l^n}(0), \\ \widehat{(\xi_\phi)}_l^n &= \mu_l\int_0^\tau \sin(\mu_l(\tau-s))\,\widehat{g_l^n}(s)ds - \frac{\tau\mu_l\sin(\mu_l\tau)}{2}\widehat{g_l^n}(0), \\ \widehat{(\dot{\xi}_\psi)}_l^n &= \int_0^\tau \cos(\beta_l(\tau-s))\,\widehat{f_l^n}(s)ds - \frac{\tau}{2}\left[\cos(\beta_l\tau)\widehat{f_l^n}(0) + \widehat{f_l^n}(\tau)\right], \\ \widehat{(\xi_\rho)}_l^n &= \mu_l\int_0^\tau \cos(\mu_l(\tau-s))\,\widehat{g_l^n}(s)ds - \frac{\tau\mu_l}{2}\left[\cos(\mu_l\tau)\widehat{g_l^n}(0) + \widehat{g_l^n}(\tau)\right]. \end{aligned}$$

Thus, the local truncation errors here are in fact the error introduced by applying the trapezoidal rule. By the standard error formula [35] of the trapezoidal rule for a general function $v(s) \in C^2[0,\tau]$, that is,

$$\int_0^\tau v(s)ds - \frac{\tau}{2}[v(0) + v(\tau)] = \frac{\tau^3}{12}v''(\kappa), \quad \text{for some } \kappa \in [0,\tau], \tag{3.18}$$

we have

$$\widehat{(\xi_\psi)}_l^n = \frac{\tau^3}{12\beta_l}[\sin(\beta_l\kappa_2)\left(\widehat{f}_l^n\right)''(\kappa_1) - 2\beta_l\cos(\beta_l\kappa_2)\left(\widehat{f}_l^n\right)'(\kappa_1) - \beta_l^2\sin(\beta_l\kappa_2)\widehat{f}_l^n(\kappa_1)], \tag{3.19a}$$

$$\widehat{(\xi_\phi)}_l^n = \frac{\tau^3\mu_l}{12}[\sin(\mu_l\kappa_2)\left(\widehat{g}_l^n\right)''(\kappa_1) - 2\mu_l\cos(\mu_l\kappa_2)\left(\widehat{g}_l^n\right)'(\kappa_1) - \mu_l^2\sin(\mu_l\kappa_2)\widehat{g}_l^n(\kappa_1)], \tag{3.19b}$$

$$\widehat{(\dot{\xi}_\psi)}_l^n = \frac{\tau^3}{12}[\cos(\beta_l\kappa_2)\left(\widehat{f}_l^n\right)''(\kappa_1) + 2\beta_l\sin(\beta_l\kappa_2)\left(\widehat{f}_l^n\right)'(\kappa_1) - \beta_l^2\cos(\beta_l\kappa_2)\widehat{f}_l^n(\kappa_1)], \tag{3.19c}$$

$$\widehat{(\xi_\rho)}_l^n = \frac{\tau^3\mu_l}{12}[\cos(\mu_l\kappa_2)\left(\widehat{g}_l^n\right)''(\kappa_1) + 2\mu_l\sin(\mu_l\kappa_2)\left(\widehat{g}_l^n\right)'(\kappa_1) - \mu_l^2\cos(\mu_l\kappa_2)\widehat{g}_l^n(\kappa_1)], \tag{3.19d}$$

for some $\kappa_2 = \tau - \kappa_1$ and $\kappa_1 \in [0, \tau]$.

Multiplying the equations in (3.19) on both sides by their complex conjugates and then using Cauchy's inequality, we get

$$\left|\widehat{(\xi_\psi)}_l^n\right|^2 \lesssim \frac{\tau^6}{\beta_l^2}\left[\left|\left(\widehat{f}_l^n\right)''(\kappa_1)\right|^2 + \beta_l^2\left|\left(\widehat{f}_l^n\right)'(\kappa_1)\right|^2 + \beta_l^4\left|\widehat{f}_l^n(\kappa_1)\right|^2\right], \tag{3.20a}$$

$$\left|\widehat{(\xi_\phi)}_l^n\right|^2 \lesssim \tau^6\mu_l^2\left[\left|\left(\widehat{g}_l^n\right)''(\kappa_1)\right|^2 + \mu_l^2\left|\left(\widehat{g}_l^n\right)'(\kappa_1)\right|^2 + \mu_l^4\left|\widehat{g}_l^n(\kappa_1)\right|^2\right], \tag{3.20b}$$

$$\left|\widehat{(\dot{\xi}_\psi)}_l^n\right|^2 \lesssim \tau^6\left[\left|\left(\widehat{f}_l^n\right)''(\kappa_1)\right|^2 + \beta_l^2\left|\left(\widehat{f}_l^n\right)'(\kappa_1)\right|^2 + \beta_l^4\left|\widehat{f}_l^n(\kappa_1)\right|^2\right], \tag{3.20c}$$

$$\left|\widehat{(\xi_\rho)}_l^n\right|^2 \lesssim \tau^6\mu_l^2\left[\left|\left(\widehat{g}_l^n\right)''(\kappa_1)\right|^2 + \mu_l^2\left|\left(\widehat{g}_l^n\right)'(\kappa_1)\right|^2 + \mu_l^4\left|\widehat{g}_l^n(\kappa_1)\right|^2\right]. \tag{3.20d}$$

Multiplying (3.20a) on both sides by $\beta_l^2 = 1 + \mu_l^2$ and then summing up for $l = 1, \ldots, N-1$, by Paserval's identity, we get

$$\|\xi_\psi^n\|_{H^1}^2 \lesssim \tau^6\left[\|\partial_{tt}f^n(\cdot,\kappa_1)\|_{L^2}^2 + \|\partial_t f^n(\cdot,\kappa_1)\|_{H^1}^2 + \|f^n(\cdot,\kappa_1)\|_{H^2}^2\right].$$

By assumption (A) and noting (3.10), we get

$$\|\xi_\psi^n\|_{H^1}^2 \lesssim \tau^6, \qquad n = 0, \ldots, \frac{T}{\tau} - 1. \tag{3.21}$$

Summing (3.20b) up directly for $l = 1, \ldots, N-1$ and noting (A) and (3.10) again, we can get

$$\|\xi_\phi^n\|_{L^2}^2 \lesssim \tau^6\left[\|\partial_{tt}g^n(\cdot,\kappa_1)\|_{H^1}^2 + \|\partial_t g^n(\cdot,\kappa_1)\|_{H^2}^2 + \|g^n(\cdot,\kappa_1)\|_{H^3}^2\right] \lesssim \tau^6, \quad n = 0, \ldots, \frac{T}{\tau} - 1. \tag{3.22}$$

Similarly for (3.20c) and (3.20d), we can get

$$\|\dot{\xi}_\psi^n\|_{L^2}^2,\ \|\xi_\rho^n\|_{L^2}^2 \lesssim \tau^6, \qquad n=0,\dots,\frac{T}{\tau}-1. \tag{3.23}$$

Combing (2.11)–(2.13) and noting (3.13), we get assertion (3.16). ∎

For the nonlinear error terms, we have estimates stated as the following lemma.

Lemma 3.4. *Based on assumption (A), and assume (3.5b) and (3.5c) hold for some* $0 \le n \le \frac{T}{\tau}-1$ *(which will be given by induction later), then we have*

$$\begin{aligned}\mathcal{E}\left(\dot{\eta}_\psi^n, \eta_\psi^n, \eta_\rho^n, \eta_\phi^n\right) \lesssim \tau^2\left[\mathcal{E}\left(\dot{e}_{\psi,N}^n, e_{\psi,N}^n, e_{\rho,N}^n, e_{\phi,N}^n\right) + \mathcal{E}\left(\dot{e}_{\psi,N}^{n+1}, e_{\psi,N}^{n+1}, e_{\rho,N}^{n+1}, e_{\phi,N}^{n+1}\right)\right]\\ + \tau^2 h^{2m_0}.\end{aligned} \tag{3.24}$$

Proof. From (3.12), we have

$$\begin{aligned}&\left|\widehat{(\eta_\psi)}_l^n\right| \lesssim \frac{\tau}{\beta_l}\left|\widehat{f}_l^n(0) - \widetilde{f}_l^n\right|, \quad \left|\widehat{(\eta_\phi)}_l^n\right| \lesssim \tau\mu_l\left|\widehat{g}_l^n(0) - \widetilde{g}_l^n\right|,\\ &\left|\widehat{(\dot{\eta}_\psi)}_l^n\right| \lesssim \tau\left[\left|\widehat{f}_l^n(0) - \widetilde{f}_l^n\right| + \left|\widehat{f}_l^n(\tau) - \widetilde{f}_l^{n+1}\right|\right], \qquad n=0,\dots,\frac{T}{\tau}-1,\\ &\left|\widehat{(\eta_\rho)}_l^n\right| \lesssim \tau\mu_l\left[\left|\widehat{g}_l^n(0) - \widetilde{g}_l^n\right| + \left|\widehat{g}_l^n(\tau) - \widetilde{g}_l^{n+1}\right|\right], \qquad l=1,\dots,N-1.\end{aligned}$$

Similarly as before, we can get for $n=0,\dots,\frac{T}{\tau}-1$,

$$\|\eta_\psi^n\|_{H^1} \lesssim \tau\|f^n(\cdot,0) - I_N f^n\|_{L^2}, \quad \|\eta_\phi^n\|_{L^2} \lesssim \tau\|g^n(\cdot,0) - g^n\|_{H^1}, \tag{3.25a}$$

$$\|\dot{\eta}_\psi^n\|_{L^2} \lesssim \tau\left[\|f^n(\cdot,0) - I_N f^n\|_{L^2} + \|f^n(\cdot,\tau) - I_N f^{n+1}\|_{L^2}\right], \tag{3.25b}$$

$$\|\eta_\rho^n\|_{L^2} \lesssim \tau\left[\|g^n(\cdot,0) - I_N g^n\|_{H^1} + \|g^n(\cdot,\tau) - I_N g^{n+1}\|_{H^1}\right]. \tag{3.25c}$$

By Lemma 3.1 and Parserval's identity, we have

$$\begin{aligned}&\|f^n(\cdot,0) - I_N f^n\|_{L^2}\\ &\lesssim \|I_N f^n(\cdot,0) - I_N f^n\|_{L^2} + \|f^n(\cdot,0) - I_N f^n(\cdot,0)\|_{L^2}\\ &\lesssim \|f^n(\cdot,0) - f^n\|_{l^2} + h^{m_0}\\ &\lesssim \|\psi(\cdot,t_n)\phi(\cdot,t_n) - \psi^n\phi^n\|_{l^2} + \||\psi|^2\psi(\cdot,t_n) - |\psi^n|^2\psi^n\|_{l^2} + h^{m_0}.\end{aligned} \tag{3.26}$$

Then by triangle inequality, under assumption (A) and (3.5b), we have

$$\begin{aligned}\|\psi(\cdot,t_n)\phi(\cdot,t_n) - \psi^n\phi^n\|_{l^2} &\lesssim \|e_\psi^n\cdot\phi(\cdot,t_n)\|_{l^2} + \|\psi^n\cdot e_\phi^n\|_{l^2}\\ &\lesssim \|e_\psi^n\|_{l^2} + \|e_\phi^n\|_{l^2} \lesssim \|e_\psi^n\|_{L^2} + \|e_\phi^n\|_{L^2}.\end{aligned}$$

Similarly,

$$\||\psi|^2\psi(\cdot,t_n) - |\psi^n|^2\psi^n\|_{l^2} \lesssim \|e_\psi^n\|_{L^2}.$$

Plugging the above two estimates back to (3.26), we get

$$\|f^n(\cdot,0) - I_N f^n\|_{L^2} \lesssim \|e_\psi^n\|_{L^2} + \|e_\phi^n\|_{L^2} + h^{m_0}. \tag{3.27}$$

Also by Lemma 3.1, we have

$$\begin{aligned}
\|g^n(\cdot,0) - I_N g^n\|_{H^1} &\lesssim \|I_N g^n(\cdot,0) - I_N g^n\|_{H^1} + \|g^n(\cdot,0) - I_N g^n(\cdot,0)\|_{H^1} \\
&\lesssim \|g^n(\cdot,0) - g^n\|_{h^1} + h^{m_0} \\
&\lesssim \||\psi(\cdot,t_n)|^2 - |\psi^n|^2\|_{h^1} + h^{m_0} \\
&\lesssim \|e_\psi^n \cdot \psi(\cdot,t_n)\|_{h^1} + \|\psi^n \cdot e_\psi^n\|_{h^1} + h^{m_0}.
\end{aligned} \tag{3.28}$$

Then with assumption (A) and Lemma 3.1,

$$\begin{aligned}
\|e_\psi^n \cdot \psi(\cdot,t_n)\|_{h^1} &\lesssim \|e_\psi^n \cdot \psi(\cdot,t_n)\|_{l^2} + \|\left(\delta_x^+ e_\psi^n\right) \cdot \psi(\cdot,t_n)\|_{l^2} + \|e_\psi^n \cdot \left(\delta_x^+ \psi(\cdot,t_n)\right)\|_{l^2} \\
&\lesssim \|e_\psi^n\|_{l^2} + \|\delta_x^+ e_\psi^n\|_{l^2} + \|e_\psi^n\|_{l^2} \lesssim \|e_\psi^n\|_{h^1} \lesssim \|e_\psi^n\|_{H^1}.
\end{aligned}$$

By assumption (3.5b) and applying the discrete Sobelov's inequality [36],

$$\begin{aligned}
\|\psi^n \cdot e_\psi^n\|_{h^1} &\lesssim \|\psi^n \cdot e_\psi^n\|_{l^2} + \|\left(\delta_x^+ e_\psi^n\right) \cdot \psi^n\|_{l^2} + \|e_\psi^n \cdot \left(\delta_x^+ \psi^n\right)\|_{l^2} \\
&\lesssim \|e_\psi^n\|_{l^2} + \|\delta_x^+ e_\psi^n\|_{l^2} + \|e_\psi^n\|_{l^\infty} \lesssim \|e_\psi^n\|_{h^1} \lesssim \|e_\psi^n\|_{H^1}.
\end{aligned}$$

Plugging the above two estimates back to (3.28), we get

$$\|g^n(\cdot,0) - I_N g^n\|_{H^1} \lesssim \|e_\psi^n\|_{H^1} + h^{m_0}. \tag{3.29}$$

As for the estimates of $\|f^n(\cdot,\tau) - I_N f^{n+1}\|_{L^2}$ and $\|g^n(\cdot,\tau) - I_N g^{n+1}\|_{H^1}$ in (3.25), following the same manner as above, we only need to show that under the induction assumptions (3.5b) and (3.5c) for some n, the numerical solutions ψ_I^{n+1} and ϕ_I^{n+1} are also bounded. In fact from the scheme (2.12), we can find

$$\|\psi_I^{n+1}\|_{H^1} \le \|\psi_I^n\|_{H^1} + \|\dot{\psi}_I^n\|_{L^2} + \frac{\tau}{2}\|I_N f^n\|_{L^2} \le 2K_1 + 2 + \|I_N f^n\|_{L^2}, \tag{3.30a}$$

$$\|\phi_I^{n+1}\|_{L^2} \le \|\phi_I^n\|_{L^2} + \|\rho_I^n\|_{L^2} + \frac{\tau}{2}\|I_N g^n\|_{H^1} \le 2K_2 + 2 + \|I_N g^n\|_{H^1}. \tag{3.30b}$$

Noting by Parserval's identity and (3.5b),

$$\begin{aligned}
&\|I_N f^n\|_{L^2} \le \|\psi^n \phi^n\|_{l^2} + \lambda \||\psi^n|^2 \psi^n\|_{l^2} \le (K_1+1)(K_2+1) + \lambda(K_1+1)^3, \\
&\|I_N g^n\|_{H^1} \le \||\psi^n|^2\|_{h^1} \le 2(K_1+1)^2,
\end{aligned}$$

which together with (3.30) show the boundedness of ψ_I^{n+1} and ϕ_I^{n+1}. Thus, similarly as before, we can get

$$\|f^n(\cdot,\tau) - I_N f^{n+1}\|_{L^2} \lesssim \|e_\psi^{n+1}\|_{L^2} + \|e_\phi^{n+1}\|_{L^2} + h^{m_0}, \tag{3.31a}$$

$$\|g^n(\cdot,\tau) - I_N g^{n+1}\|_{H^1} \lesssim \|e_\psi^{n+1}\|_{H^1} + h^{m_0}. \tag{3.31b}$$

At last, plugging (3.27, 3.29), and (3.31) back to (3.25), and noticing by applying the projection and triangle inequality,

$$\|e_\psi^n\|_{H^1} \le \|e_{\psi,N}^n\|_{H^1} + \|\psi(\cdot,t_n) - \psi_N(\cdot,t_n)\|_{H^1} \lesssim \|e_{\psi,N}^n\|_{H^1} + h^{m_0},$$
$$\|e_\phi^n\|_{L^2} \le \|e_{\phi,N}^n\|_{L^2} + \|\phi(\cdot,t_n) - \phi_N(\cdot,t_n)\|_{L^2} \lesssim \|e_{\phi,N}^n\|_{L^2} + h^{m_0}, \quad n = 0,\ldots,\frac{T}{\tau}.$$

so we have

$$\|\eta_\psi^n\|_{H^1} \lesssim \tau\left[\|e_{\psi,N}^n\|_{H^1} + \|e_{\phi,N}^n\|_{L^2} + h^{m_0}\right], \quad \|\eta_\phi^n\|_{L^2} \lesssim \tau\left[\|e_{\psi,N}^n\|_{H^1} + h^{m_0}\right],$$
$$\|\dot\eta_\psi^n\|_{L^2} \lesssim \tau\left[\|e_{\psi,N}^n\|_{H^1} + \|e_{\phi,N}^n\|_{L^2} + \|e_{\psi,N}^{n+1}\|_{H^1} + \|e_{\phi,N}^{n+1}\|_{L^2} + h^{m_0}\right],$$
$$\|\eta_\rho^n|_{L^2} \lesssim \tau\left[\|e_{\psi,N}^n\|_{H^1} + \|e_{\psi,N}^{n+1}\|_{H^1} + h^{m_0}\right], \qquad n = 0,\ldots,\frac{T}{\tau} - 1.$$

Then by (3.13) and Cauchy's inequality, we get

$$\begin{aligned}\mathcal{E}\left(\dot\eta_\psi^n, \eta_\psi^n, \eta_\rho^n, \eta_\phi^n\right) &\lesssim \tau^2\left[\|e_{\psi,N}^n\|_{H^1}^2 + \|e_{\phi,N}^n\|_{L^2}^2 + \|e_{\psi,N}^{n+1}\|_{H^1}^2 + \|e_{\phi,N}^{n+1}\|_{L^2}^2\right] + \tau^2 h^{2m_0}\\ &\lesssim \tau^2\left[\mathcal{E}\left(\dot e_{\psi,N}^n, e_{\psi,N}^n, e_{\rho,N}^n, e_{\phi,N}^n\right) + \mathcal{E}\left(\dot e_{\psi,N}^{n+1}, e_{\psi,N}^{n+1}, e_{\rho,N}^{n+1}, e_{\phi,N}^{n+1}\right)\right] + \tau^2 h^{2m_0}.\end{aligned}$$

and we complete the proof. ∎

With the error energy functional notation (3.13), we are ready to show the following fact.

Lemma 3.5. *For $n = 0,\ldots,\frac{T}{\tau} - 1$, we have*

$$\begin{aligned}&\mathcal{E}\left(\dot e_{\psi,N}^{n+1}, e_{\psi,N}^{n+1}, e_{\rho,N}^{n+1}, e_{\phi,N}^{n+1}\right) - \mathcal{E}\left(\dot e_{\psi,N}^n, e_{\psi,N}^n, e_{\rho,N}^n, e_{\phi,N}^n\right)\\ &\quad\lesssim \tau\mathcal{E}\left(\dot e_{\psi,N}^n, e_{\psi,N}^n, e_{\rho,N}^n, e_{\phi,N}^n\right) + \frac{1}{\tau}\left[\mathcal{E}\left(\dot\xi_\psi^n, \xi_\psi^n, \xi_\rho^n, \xi_\phi^n\right) + \mathcal{E}\left(\dot\eta_\psi^n, \eta_\psi^n, \eta_\rho^n, \eta_\phi^n\right)\right]. \end{aligned} \tag{3.33}$$

Proof. Multiplying the equations in (3.11) on both sides by their complex conjugates and applying Cauchy's inequality, we get

$$\begin{aligned}\left|\widehat{(e_\psi)}_l^{n+1}\right|^2 &\le (1+\tau)\left|\cos(\beta_l\tau)\,\widehat{(e_\psi)}_l^n + \frac{\sin(\beta_l\tau)}{\beta_l}\widehat{(\dot e_\psi)}_l^n\right|^2\\ &\quad + \left(1+\frac{1}{\tau}\right)\left|\widehat{(\xi_\psi)}_l^n - \widehat{(\eta_\psi)}_l^n\right|^2, \end{aligned}\tag{3.34a}$$

$$\begin{aligned}\left|\widehat{(e_\phi)}_l^{n+1}\right|^2 &\le (1+\tau)\left|\cos(\mu_l\tau)\,\widehat{(e_\phi)}_l^n + \sin(\mu_l\tau)\,\widehat{(e_\rho)}_l^n\right|^2\\ &\quad + \left(1+\frac{1}{\tau}\right)\left|\widehat{(\xi_\phi)}_l^n - \widehat{(\eta_\phi)}_l^n\right|^2, \end{aligned}\tag{3.34b}$$

$$\begin{aligned}\left|\widehat{(\dot e_\psi)}_l^{n+1}\right|^2 &\le (1+\tau)\left|-\beta_l\sin(\beta_l\tau)\,\widehat{(e_\psi)}_l^n + \cos(\beta_l\tau)\,\widehat{(\dot e_\psi)}_l^n\right|^2\\ &\quad + \left(1+\frac{1}{\tau}\right)\left|\widehat{(\dot\xi_\psi)}_l^n - \widehat{(\dot\eta_\psi)}_l^n\right|^2, \end{aligned}\tag{3.34c}$$

$$\left|\widehat{(e_\rho)}_l^{n+1}\right|^2 \le (1+\tau)\left|-\sin(\mu_l\tau)\,\widehat{(e_\phi)}_l^n + \cos(\mu_l\tau)\,\widehat{(e_\rho)}_l^n\right|^2 + \left(1+\frac{1}{\tau}\right)\left|\widehat{(\xi_\rho)}_l^n - \widehat{(\eta_\rho)}_l^n\right|^2, \tag{3.34d}$$

Multiplying (3.34a) by β_l^2 and then adding to (3.34c), we get

$$\left(1+\mu_l^2\right)|\widehat{(e_\psi)}_l^{n+1}|^2 + |\widehat{(\dot e_\psi)}_l^{n+1}|^2 \le (1+\tau)\left[\left(1+\mu_l^2\right)|\widehat{(e_\psi)}_l^n|^2 + |\widehat{(\dot e_\psi)}_l^n|^2\right] + \left(1+\frac{1}{\tau}\right) \times \left[\left(1+\mu_l^2\right)|\widehat{(\xi_\psi)}_l^n - \widehat{(\eta_\psi)}_l^n|^2 + |\widehat{(\dot\xi_\psi)}_l^n - \widehat{(\dot\eta_\psi)}_l^n|^2\right]. \tag{3.35}$$

Adding (3.34b) to (3.34d), we get

$$|\widehat{(e_\phi)}_l^{n+1}|^2 + |\widehat{(e_\rho)}_l^{n+1}|^2 \le (1+\tau)\left[|\widehat{(e_\phi)}_l^n|^2 + |\widehat{(e_\rho)}_l^n|^2\right] + \left(1+\frac{1}{\tau}\right)\left[|\widehat{(\xi_\phi)}_l^n - \widehat{(\eta_\phi)}_l^n|^2 + |\widehat{(\xi_\rho)}_l^n - \widehat{(\eta_\rho)}_l^n|^2\right]. \tag{3.36}$$

Adding (3.35) to (3.36), and then summing up for $l = 1, \ldots, N-1$, noting (3.13), we get

$$\mathcal{E}\left(\dot e_{\psi,N}^{n+1}, e_{\psi,N}^{n+1}, e_{\rho,N}^{n+1}, e_{\phi,N}^{n+1}\right) \le (1+\tau)\mathcal{E}\left(\dot e_{\psi,N}^n, e_{\psi,N}^n, e_{\rho,N}^n, e_{\phi,N}^n\right) + \left(1+\frac{1}{\tau}\right)\mathcal{E}\left(\dot\xi_\psi^n - \dot\eta_\psi^n, \xi_\psi^n - \eta_\psi^n, \xi_\rho^n - \eta_\rho^n, \xi_\phi^n - \eta_\phi^n\right),$$

which with triangle inequality prove assertion (3.33). ∎

Now, combining the Lemmas 3.2 3.3 3.4, we give the proof of Theorem 3.1 by energy method with the help of mathematical induction argument [9, 21], or the equivalent cutoff technique [37, 38] for the boundedness of numerical solutions.

Proof of Theorem 3.1. $n = 0$, from the scheme and assumption (A), we have

$$\begin{aligned}&||\dot e_\psi^0||_{L^2} + ||e_\psi^0||_{H^1} + ||e_\phi^0||_{L^2}\\ &\quad \lesssim ||\psi^{(1)} - I_N\psi^{(1)}||_{L^2} + ||\psi^{(0)} - I_N\psi^{(0)}||_{H^1} + ||\phi^{(0)} - I_N\phi^{(0)}||_{L^2} \lesssim h^{m_0},\end{aligned}$$

Moreover, noting (3.4, 3.3), and (3.8), we get

$$||e_\rho^0||_{L^2} \lesssim ||\phi^{(1)} - I_N\phi^{(1)}||_{L^2} \lesssim h^{m_0}.$$

Then by triangle inequality,

$$\begin{aligned}||\psi_I^n||_{H^1} &\le ||\psi(\cdot,t_n)||_{H^1} + ||e_\psi^n||_{H^1} \le K_1 + 1,\\ ||\phi_I^n||_{L^2} &\le ||\phi(\cdot,t_n)||_{L^2} + ||e_\phi^n||_{L^2} \le K_2 + 1,\end{aligned}$$

$$||\dot{\psi}_I^n||_{L^2} \leq ||\partial_t \psi(\cdot, t_n)||_{L^2} + ||\dot{e}_\psi^n||_{L^2} \leq K_1 + 1,$$
$$||\rho_I^n||_{L^2} \leq ||\partial_x \varphi(\cdot, t_n)||_{L^2} + ||e_\rho^n||_{L^2} \leq K_2 + 1,$$

for $0 < h \leq h_1$, where h_1 is a constant independent of τ and h. Obviously, $||\psi^0||_{l^\infty} \leq K_1 + 1$. Thus (3.5) is true for $n = 0$.

Assume (3.5) is valid for $n \leq M \leq T/\Delta t - 1$. Now we need to show the results still hold for $n = M + 1$. First of all, by triangle inequality and projection error estimate with assumption (A), we have

$$\begin{aligned} &||\dot{e}_\psi^{M+1}||_{L^2} + ||e_\psi^{M+1}||_{H^1} + ||e_\rho^{M+1}||_{L^2} + ||e_\phi^{M+1}||_{L^2} \\ &\lesssim ||\dot{e}_{\psi,N}^{M+1}||_{L^2} + ||e_{\psi,N}^{M+1}||_{H^1} + ||e_{\rho,N}^{M+1}||_{L^2} + ||e_{\phi,N}^{M+1}||_{L^2} + h^{m_0}. \end{aligned} \tag{3.37}$$

As (3.5b) and (3.5c) are assumed to be true under induction for all $n \leq N$, so we can plug the estimates (3.16) from Lemma 3.2 and (3.24) from Lemma 3.3 into (3.33) and get for $n = 0, \ldots, M$,

$$\begin{aligned} &\mathcal{E}\left(\dot{e}_{\psi,N}^{n+1}, e_{\psi,N}^{n+1}, e_{\rho,N}^{n+1}, e_{\phi,N}^{n+1}\right) - \mathcal{E}\left(\dot{e}_{\psi,N}^{n}, e_{\psi,N}^{n}, e_{\rho,N}^{n}, e_{\phi,N}^{n}\right) \\ &\lesssim \tau\left[\mathcal{E}\left(\dot{e}_{\psi,N}^{n+1}, e_{\psi,N}^{n+1}, e_{\rho,N}^{n+1}, e_{\phi,N}^{n+1}\right) + \mathcal{E}\left(\dot{e}_{\psi,N}^{n}, e_{\psi,N}^{n}, e_{\rho,N}^{n}, e_{\phi,N}^{n}\right)\right] + \tau^5 + \tau \cdot h^{2m_0}. \end{aligned} \tag{3.38}$$

Summing (3.38) up for $n = 0, 1, \ldots, M$, and then by the discrete Gronwall's inequality, we get

$$\mathcal{E}\left(\dot{e}_{\psi,N}^{n+1}, e_{\psi,N}^{n+1}, e_{\rho,N}^{n+1}, e_{\phi,N}^{n+1}\right) \lesssim \tau^4 + h^{2m_0}.$$

Thus, we have

$$||\dot{e}_{\psi,N}^{M+1}||_{L^2} + ||e_{\psi,N}^{M+1}||_{H^1} + ||e_{\rho,N}^{M+1}||_{L^2} + ||e_{\phi,N}^{M+1}||_{L^2} \lesssim \tau^2 + h^{m_0},$$

which together with (3.37) show that (3.5b) is valid for $n = M + 1$. Then by triangle inequality,

$$\begin{aligned} &||\psi_I^{M+1}||_{H^1} \leq ||\psi(\cdot, t_{M+1})||_{H^1} + ||e_\psi^{M+1}||_{H^1} \leq K_1 + 1, \\ &||\phi_I^{M+1}||_{L^2} \leq ||\phi(\cdot, t_{M+1})||_{L^2} + ||e_\phi^{M+1}||_{L^2} \leq K_2 + 1, \\ &||\dot{\psi}_I^{M+1}||_{L^2} \leq ||\partial_t \psi(\cdot, t_{M+1})||_{L^2} + ||\dot{e}_\psi^{M+1}||_{H^1} \leq K_1 + 1, \\ &||\rho_I^{M+1}||_{L^2} \leq ||\partial_x \varphi(\cdot, t_{M+1})||_{L^2} + ||e_\rho^{M+1}||_{L^2} \leq K_2 + 1, \quad 0 < \tau \leq \tau_1, 0 < h \leq h_2, \end{aligned}$$

for some constants τ_1, $h_2 > 0$ independent of τ and h. Noting the Sobolev's inequality

$$||e_\psi^{M+1}||_{L^\infty} \lesssim ||e_\psi^{M+1}||_{H^1},$$

we also have

$$||\psi^{M+1}||_{l^\infty} \leq ||\psi_I^{M+1}||_{L^\infty} \leq ||\psi(\cdot, t_{M+1})||_{L^\infty} + ||e_\psi^{M+1}||_{L^\infty} \leq K_1 + 1,$$

for $0 < \tau \leq \tau_2$, $0 < h \leq h_3$, where $\tau_2, h_3 > 0$ are two constants independent of τ and h. Therefore, the proof is completed by choosing $\tau_0 = \min\{\tau_1, \tau_2\}$ and $h_0 = \min\{h_1, h_2, h_3\}$. ∎

Remark 3.6. We would like to remark that although the error estimate arguments are given for 1 D, the results and proof for higher dimensions can be achieved in the same spirit. In higher dimensional space, the Sobolev's inequality reads $||v||_{L^\infty} \lesssim ||v||_{H^2}$, for some $v \in H^2$. If we still work in the energy space $H^1 \times L^2$ for ψ and ϕ, respectively in 2D/3D, due to the use of the inverse inequality to provide the bound in l^∞-norm of the numerical solution [9, 33, 37], we need impose the technical condition

$$\tau \lesssim \rho_d(h), \quad \text{with} \quad \rho_d(h) = \begin{cases} 1/\sqrt{|\ln h|}, & d = 2, \\ h^{1/4}, & d = 3, \end{cases} \tag{3.39}$$

to get the error estimates. Of course, if the solution of the KGZ is smooth enough, we can always rise the energy space for error functions to $H^2 \times H^1$, under a stronger regularity assumption than (A). Then there will be no need to assume the stability (or CFL-type) condition (3.39).

Remark 3.7. The EWI-SP method and the analysis can be easily extended to to the study the generalized KGZ system [4, 10],

$$\begin{aligned} &\partial_{tt}\psi(\mathbf{x},t) - \Delta\psi(\mathbf{x},t) + \psi(\mathbf{x},t) + \psi(\mathbf{x},t)\phi(\mathbf{x},t) + f\left(|\psi(\mathbf{x},t)|^2\right)\psi(\mathbf{x},t) = 0, \\ &\partial_{tt}\phi(\mathbf{x},t) - \Delta\phi(\mathbf{x},t) - \Delta\left(g\left(|\psi(\mathbf{x},t)|^2\right)\right) = 0, \quad \mathbf{x} \in \mathbb{R}^d, \quad t > 0, \end{aligned}$$

for some general function $f(\cdot), g(\cdot)$ defined on $\mathbb{R}$. All the results presented in this work remain valid, provided f, g are smooth enough.

Remark 3.8. By the convergence theorem, we claim that the CFL-type condition required in [9] is not needed for the proposed EWI-SP method. Note that the usual CFL condition refers to the constraint on time step and mesh size to guarantee the absolute stability or strong stability of numerical methods [24], which can only be obtained by the linear or von Neumann stability analysis. Here the CFL-type constraint we are referring to is the condition required by the finite time error estimate to provide the finite time convergence of numerical methods, that is, the practical stability condition [24]. We do not claim the proposed EWI-SP is absolutely stable without any conditions theoretically, though numerically it appears to be as shall be seen in the next section.

IV. NUMERICAL RESULTS

In this section, we shall test the proposed EWI-SP method and report the numerical results to confirm our theoretical studies. Comparisons with the GISP method are included. The errors presented here are measured under the same energy norm as used the (3.5), that is, $||e_\psi||_{H^1}$, $||e_\phi||_{L^2}$, $||\dot{e}_\psi||_{L^2}$ and $||e_\rho||_{L^2}$ for variables ψ, ϕ, $\partial_t\psi$, and $\partial_t\phi$, respectively.

A. Convergence Test

Example 4.1. To first test the convergence and accuracy of the EWI-SP, we consider the soliton solutions in the 1D KGZ (1.1) where the analytical expressions of the solutions are known [3, 4]:

$$\begin{aligned} &\psi_S(x,t) = \sqrt{A(v^2-1)} \cdot \operatorname{sech}\left(B(x + x_0 - vt)\right) \cdot \exp\left(i\omega(t - vx - vx_0)\right), \\ &\phi_S(x,t) = A \cdot \operatorname{sech}(B(x + x_0 - vt))^2, \quad x \in \mathbb{R},\, t \geq 0, \end{aligned}$$

where

$$B=\sqrt{\frac{(\lambda-1)A-\lambda v^2A}{2(1-v^2)}},\qquad \omega=\sqrt{\frac{2+\lambda v^2A+(1-\lambda)A}{2(1-v^2)}},$$

with $x_0\in\mathbb{R}$ the shift in space, and the parameters $v,\ A\in\mathbb{R}$ chosen such that the width B and frequency ω are real. Here, we choose

$$\lambda=1,\quad A=-3,\quad v=0.8, \tag{4.1}$$

with the shift $x_0=1.5$. Then we take the initial data in (2.1) as

$$\begin{aligned}
&\psi^{(0)}(x)=\psi_S(x,t=0),\quad \phi^{(0)}(x)=\phi_S(x,t=0),\\
&\psi^{(1)}(x)=\partial_t\psi_S(x,t=0)\\
&\qquad=\sqrt{A(v^2-1)}\cdot\operatorname{sech}(B(x+x_0))\cdot\exp(-i\omega v(x+x_0))\cdot[Bv\cdot\tanh(B(x+x_0))+i\omega],\\
&\phi^{(1)}(x)=\partial_t\phi_S(x,t=0)=2ABv\cdot\operatorname{sech}(B(x+x_0))^2\cdot\tanh(B(x+x_0)).
\end{aligned}$$

Choosing the computational domain $\Omega=[-16,16]$, that is, $b=-a=16$ in (2.1), which is large enough to neglect the truncation error by the zero boundary conditions, we solve the KGZ (2.1) numerically by the EWI-SP (2.11)–(2.13) before the solitons get close to the boundary. To study the error bounds, we test the spatial and temporal discretization errors of the EWI-SP separately. First, for the discretization error in space, we take a very small time step $\tau=10^{-5}$ such that the error from the discretization in time is negligible compared with the spatial discretization error. The errors are presented at $T=3$ and tabulated in Table I. The results here for the EWI-SP are totally same as the spatial error of the GISP method (2.19)–(2.20), as both methods have the same spatial discretization. Second, for the discretization error in time, we take a fine mesh size $h=1/16$ such that the error from the discretization in space is negligible compared with the temporal discretization error. The errors together with computational time are presented at $T=3$ and tabulated in Table II including comparisons with the GISP method. The computations are done on a laptop via Matlab. To test the stability and further justify the CFL-free type convergence, the temporal error of the EWI-SP at $T=10$ via large time steps under a very small mesh size $h=2^{-12}$ are shown in Fig. 1.

Example 4.2. To guarantee different frequencies are presented in the solution, in our second numerical example we consider initial data as

$$\psi^{(0)}(x)=\left(1+\frac{i}{2}\right)\frac{e^{-x^2}}{1+\sin^2(x)},\quad \psi^{(1)}(x)=\frac{\pi}{3}\operatorname{sech}(\sqrt{2}x^2),$$
$$\phi^{(0)}(x)=\operatorname{sech}(x^2)\cos\left(\sqrt{3}x\right),\quad \phi^{(1)}(x)=\left(\frac{1}{2}+i\right)\frac{e^{-2x^2}}{1+x^2}.$$

We choose the same computational domain $\Omega=[-16,16]$ for Example 4.2. In this case, as the analytical solution is not available, so the "'exact"' solution is obtained numerically by the EWI-SP method (2.11)–(2.13) with very small time step and mesh size, for example, $\tau=10^{-5}, h=1/64$.

TABLE I. Example 4.1: spatial error analysis of EWI-SP for different h at time $T = 3$ under $\tau = 10^{-5}$.

EWI-SP	$h_0 = 1$	$h_0/2$	$h_0/4$	$h_0/8$
$\|e_\psi^n\|_{H^1}$	5.65 E −01	6.48 E −02	3.64 E −04	2.91 E −09
$\|e_\phi^n\|_{L^2}$	9.01 E −01	9.45 E −02	4.79 E −04	3.77 E −09
$\|\dot{e}_\psi^n\|_{L^2}$	5.80 E −01	5.73 E −02	3.61 E −04	2.83 E −09
$\|e_\rho^n\|_{L^2}$	2.02 E+00	8.88 E −02	4.76 E −04	3.63 E −09

TABLE II. Example 4.1: temporal error analysis of EWI-SP and comparisons with GISP for different τ at time $T = 3$ under $h = 1/16$ including computational time (seconds).

EWI-SP	$\tau_0 = 0.2$	$\tau_0/2$	$\tau_0/4$	$\tau_0/8$	$\tau_0/16$
$\|e_\psi^n\|_{H^1}$	3.25 E −02	8.10 E −03	2.00 E −03	5.10 E −04	1.27 E −04
$\|e_\phi^n\|_{L^2}$	4.91 E −02	1.23 E −02	3.10 E −03	7.70 E −04	1.93 E −04
$\|\dot{e}_\psi^n\|_{L^2}$	2.32 E −02	5.70 E −03	1.40 E −03	3.58 E −04	8.94 E −05
$\|e_\rho^n\|_{L^2}$	3.80 E −02	9.50 E −03	2.40 E −03	5.90 E −04	1.47 E −04
Time	0.016	0.031	0.063	0.11	0.23
GISP	$\tau_0 = 0.2$	$\tau_0/2$	$\tau_0/4$	$\tau_0/8$	$\tau_0/16$
$\|e_\psi^n\|_{H^1}$	4.14 E −02	9.70 E −03	2.40 E −03	5.98 E −04	1.49 E −04
$\|e_\phi^n\|_{L^2}$	6.27 E −02	1.48 E −02	3.70 E −03	9.14 E −04	2.28 E −04
$\|\dot{e}_\psi^n\|_{L^2}$	4.28 E −02	1.02 E −02	2.50 E −03	6.31 E −04	1.58 E −04
$\|e_\rho^n\|_{L^2}$	6.38 E −02	1.53 E −02	3.80 E −03	9.47 E −04	2.37 E −04
Time	0.016	0.031	0.047	0.078	0.19

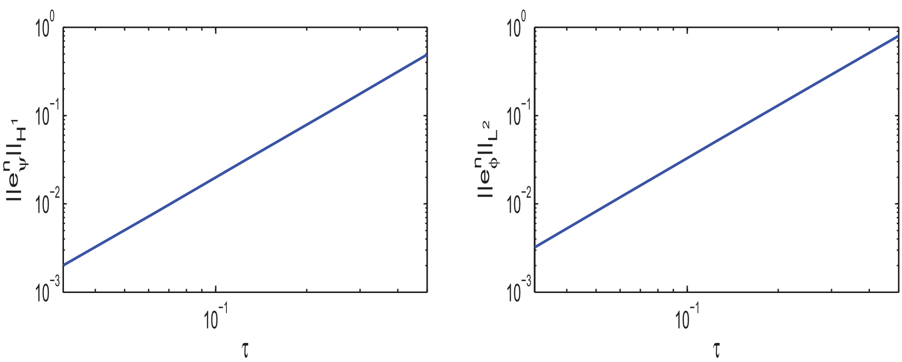

FIG. 1. Temporal error of Example 4.1 in log-scale: $||e_\psi^n||_{H^1}$ (left) and $||e_\phi^n||_{L^2}$ (right) under a very small mesh size $h = 2^{-12}$ at time $T = 10$. [Color figure can be viewed in the online issue, which is available at wileyonlinelibrary.com.]

Again the spatial errors of DISP at $T = 3$ are tabulated in Table III, and the temporal errors including comparisons with GISP are tabulated in Table IV. Moreover, the errors of both EWI-SP and GISP at $T = 10$ with some large time steps under different mesh size are given in Table V.

B. Long-Time Energy Conservation

To validating the scheme furthermore, we test the energy conservation law (1.3) in the Example 4.1 by using the EWI-SP. Choose the same parameters (4.1), but with an enlarged domain

TABLE III. Example 4.2: spatial error analysis of EWI-SP for different h at time $T = 3$ under $\tau = 10^{-5}$.

EWI-SP	$h_0 = 1$	$h_0/2$	$h_0/4$	$h_0/8$
$\|e_\psi^n\|_{H^1}$	5.23 E −01	4.51 E −02	3.91 E −04	6.29 E −08
$\|e_\phi^n\|_{L^2}$	5.44 E −01	8.07 E −02	7.91 E −04	7.81 E −08
$\|\dot{e}_\psi^n\|_{L^2}$	4.12 E −01	5.50 E −02	9.88 E −04	3.90 E −08
$\|e_\rho^n\|_{L^2}$	4.51 E+00	1.66 E −01	1.00 E −03	5.10 E −08

TABLE IV. Example 4.2: temporal error analysis of EWI-SP and comparisons with GISP for different τ at time $T = 3$ under $h = 1/16$ including computational time (seconds).

EWI-SP	$\tau_0 = 0.2$	$\tau_0/2$	$\tau_0/4$	$\tau_0/8$	$\tau_0/16$
$\|e_\psi^n\|_{H^1}$	1.01 E −02	2.30 E −03	5.56 E −04	1.38 E −04	3.45 E −05
$\|e_\phi^n\|_{L^2}$	4.91 E −02	1.23 E −02	3.10 E −03	7.70 E −04	1.93 E −04
$\|\dot{e}_\psi^n\|_{L^2}$	2.32 E −02	5.70 E −03	1.40 E −03	3.58 E −04	8.94 E −05
$\|e_\rho^n\|_{L^2}$	3.80 E −02	9.50 E −03	2.40 E −03	5.90 E −04	1.47 E −04
Time	0.016	0.031	0.063	0.13	0.23
GISP	$\tau_0 = 0.2$	$\tau_0/2$	$\tau_0/4$	$\tau_0/8$	$\tau_0/16$
$\|e_\psi^n\|_{H^1}$	5.14 E −02	9.70 E −03	2.30 E −03	5.80 E −04	1.45 E −04
$\|e_\phi^n\|_{L^2}$	5.55 E −02	1.15 E −02	2.80 E −03	6.96 E −04	1.74 E −04
$\|\dot{e}_\psi^n\|_{L^2}$	7.84 E −02	1.38 E −02	3.30 E −03	8.24 E −04	2.06 E −04
$\|e_\rho^n\|_{L^2}$	9.16 E −02	1.63 E −02	4.00 E −03	9.82 E −04	2.45 E −04
Time	0.016	0.031	0.047	0.094	0.16

TABLE V. Example 4.2: the error $\|e_\psi^n\|_{H^1} + \|e_\phi^n\|_{L^2}$ of EWI-SP and GISP for some large τ at time $T = 10$ under different h.

EWI-SP	$\tau_0 = 0.5$	$\tau_0/2$	$\tau_0/4$	$\tau_0/8$	$\tau_0/16$
$h_0 = 0.5$	1.13 E+00	1.67 E −01	1.01 E −01	9.37 E −02	9.28 E −02
$h_0/2^1$	1.07 E+00	1.65 E −01	3.37 E −02	9.10 E −03	3.90 E −03
$h_0/2^2$	1.07 E+00	1.67 E −01	3.35 E −02	8.30 E −03	2.10 E −03
$h_0/2^{11}$	1.07 E+00	1.67 E −01	3.35 E −02	8.30 E −03	2.10 E −03
GISP	$\tau_0 = 0.5$	$\tau_0/2$	$\tau_0/4$	$\tau_0/8$	$\tau_0/16$
$h_0 = 0.5$	Unstable	3.72 E −01	1.31 E −01	9.68 E −02	9.32 E −02
$h_0/2^1$	Unstable	Unstable	8.68 E −02	2.16 E −02	6.50 E −03
$h_0/2^2$	Unstable	Unstable	Unstable	2.14 E −02	5.30 E −03
$h_0/2^{11}$	Unstable	Unstable	Unstable	2.26 E+03	Unstable

$\Omega = [-256, 256]$ and shift $x_0 = 240$ to provide a long-time simulation without significant boundary truncation error. The EWIs in general are not conservative schemes like those in [1, 38], as the nonlinearities in the differential equations are not integrated in a conservative form. In general, we remark it would be very challenging to propose a conservative EWI. Thus, we do not expect an "energy" that is conserved in the discrete level by the EWI-SP. Instead, we compute the numerical energy

$$E^n := \int_\Omega \Big[|\dot{\psi}_I^n|^2 + |\frac{d}{dx}\psi_I^n|^2 + |\psi_I^n|^2 + \frac{1}{2}|\rho_I^n|^2 + \frac{1}{2}|\phi_I^n|^2 + I_N\left(\phi^n \cdot |\psi^n|^2\right) \\ + \frac{\lambda}{2} I_N\left(|\psi^n|^4\right) \Big] dx, \tag{4.2}$$

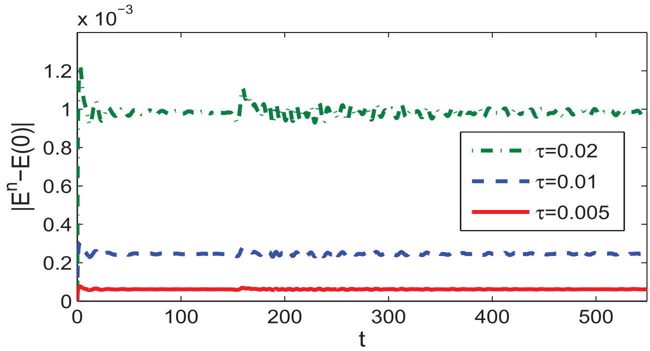

FIG. 2. Time evolution of the energy fluctuations: $|E^n - E(0)|$ under different time step τ and mesh size $h = 1/16$ till $T = 550$. [Color figure can be viewed in the online issue, which is available at wileyonlinelibrary.com.]

with the numerical solutions given by EWI-SP and the notations here introduced in (3.2)–(3.3). Figure 2 shows time evolution of the error between the exact energy (1.3) and the numerical energy (4.2) under different time step τ and a fixed mesh size $h = 1/16$, where the exact energy is obtained from the initial data $E(t = 0)$ with a very fine mesh $h = 1/16$ for the spectral approximations of the spatial derivative.

From Tables I–V, Figs. 1 and 2 and additional results not shown here brevity, we can draw the following observations:

1. The EWI-SP method (2.11)–(2.13) is of spectral accuracy in space (cf. Tables I and III), and is of second-order accuracy in time (cf. Tables II and IV), which confirms the theoretical error estimates (3.5) and indicates the error bound there is optimal.
2. The EWI-SP method is very stable and allows use of large time steps and mesh size, while the GISP suffers from a CFL-type stability condition (cf. Fig. 1 and Table V). The numerical performance of EWI-SP is better than GISP from both stability and accuracy points of view, while the computational costs of both methods are very close (cf. Tables II and IV).
3. The EWI-SP method conserves the energy (1.3) very well during the computations. Although EWI-SP is not a conservative scheme, the numerical energy is just small fluctuation from the exact energy during the long time simulation, and will converge to the exact energy when time step decreases (Fig. 2).

V. CONCLUSION

In this work, we proposed and analyzed an exponential wave integrator sine pseudospectral (EWI-SP) method for solving the Klein–Gordon–Zakharov (KGZ) system, which is a classical model to describe the interactions between the Langmuir waves and ion acoustic waves in a plasma. The numerical method here is based on a Deuflhard-type exponential wave integrator for temporal integrations and the sine pseudospectral method for spatial discretizations. The scheme is fully explicit, time reversible and very efficient due to the fast discrete sine transform. Using correct energy spaces, rigorous finite time error estimate results of the EWI-SP method were established without any CFL-type conditions. The results indicate that the method has second-order accuracy in time and spectral accuracy in space. Extensive numerical experiments were carried out to confirm the theoretically studies. Numerical results and comparisons suggest the EWI-SP is very stable, more accurate than the existing method and allow to use large time steps and mesh size in practical computing.

References

1. T. Wang, J. Chen, and L. Zhang, Conservative difference methods for the Klein-Gordon-Zakharov equations, J Comput App Math 205 (2007), 430–452.
2. J. Chen and L. Zhang, Numerical simulation for the initial-boundary value problem of the Klein-Gordon-Zakharov equations, Acta Math Appl Sin 28 (2012), 325–336.
3. M. Dehghan and A. Nikpour, The solitary wave solution of coupled Klein-Gordon-Zakharov equations via two different numerical methods, Comput Phys Comm 184 (2013), 2145–2158.
4. M. Ismaila and A. Biswas, 1-Soliton solution of the Klein-Gordon-Zakharov equation with power law nonlinearity, Appl Math Comput 217 (2010), 4186–4196.
5. M. Colin and T. Colin, On a quasilinear Zakharov sytem describing laser-plasma intercations, Differential Integral Equations 17 (2004), 297–330.
6. B. Texier, WKB asymptotics for the Euler-Maxwell equations, Asymptot Anal 42 (2005), 211–250.
7. P. Bellan, Fundamentals of plasmas physics, Cambridge University Press, Cambridge, 2006.
8. R. Dendy, Plasma dynamics, Oxford University Press, Oxford, 1990.
9. W. Bao and X. Dong, Analysis and comparison of numerical methods for the Klein-Gordon equation in the nonrelativistic limit regime, Numer Math 120 (2012), 189–229.
10. H. Triki and N. Boucerredj, Soliton solutions of the Klein-Gordon-Zakharov equations with power law nonlinearity, Appl Math Comput 227 (2014), 341–346.
11. B. Guo and G. Yuan, Global smooth solution for the Klein-Gordon-Zakharov equations, J Math Phys 36 (1995), 4119–4124.
12. K. Tsutaya, Global existence of small amplitude solutions for the Klein-Gordon-Zakharov equations, Nonlinear Anal 27 (1996), 1373–1380.
13. T. Ozawa, K. Tsutaya, and Y. Tsutsumi, Well-posedness in energy space for the Cauchy problem of the Klein-Gordon-Zakharov equations with different propagation speeds in three space dimensions, Math Ann 313 (1999), 127–140.
14. N. Masmoudi and K. Nakanishi, From the Klein-Gordon-Zakharov system to the nonlinear Schrödinger equation, J Hyperbolic Differential Equations 2 (2005), 975–1008.
15. N. Masmoudi and K. Nakanishi, Energy convergence for singular limits of Zakharov type systems, Invent Math 172 (2008), 535–583.
16. D. Cohen, Conservation properties of numerical integrators for highly oscillatory Hamiltonian systems, IMA J Numer Anal 26 (2005), 34–59.
17. E. Hairer, Ch. Lubich, and G. Wanner, Geometric numerical integration, Springer-Verlag, Berlin Heidelberg, 2002.
18. E. Hairer and Ch. Lubich, Long-time energy conservation of numerical methods for oscillatory differential equations, SIAM J Numer Anal 38 (2000), 414–441.
19. M. Ablowitz, M. Kruskal, and J. Ladik, Solitary wave collisions, SIAM J Appl Math 36 (1979), 428–437.
20. M. Ghoreishi, A. Ismail, and A. Rashidy, Numerical solution of Klein-Gordon-Zakharov equations using Chebyshev Cardinal functions, J Comput Anal Appl 14 (2012), 574–582.
21. W. Bao, X. Dong and X. Zhao, An exponential wave integrator pseudospectral method for the Klein-Gordon-Zakharov system, SIAM J Sci Comput 35 (2013), A2903–A2927.

22. W. Gautschi, Numerical integration of ordinary differential equations based on trigonometric polynomials, Numer Math 3 (1961), 381–397.

23. M. Hochbruck and Ch. Lubich, A Gautschi-type method for oscillatory second-order differential equations, Numer Math 83 (1999), 402–426.

24. K.W. Morton and D.F. Mayers, Numerical solution of partial differential equations, 2nd Ed., Cambridge University Press, Cambridge, 2005.

25. P. Deuflhard, A study of extrapolation methods based on multistep schemes without parasitic solutions, ZAMP, 30 (1979), 177–189.

26. V. Zakharov, Collapse of Langmuir waves, Sov J Exp Theor Phys 35 (1972), 908–914.

27. W. Bao and L. Yang, Efficient and accurate numerical methods for the Klein-Gordon-Schrodinger equations, J Comput Phys 225 (2007), 1863–1893.

28. B. Engquist and A. Majda, Absorbing boundary conditions for numerical simulation of waves, Proc Natl Acad Sci USA 75 (1977), 1765–1766.

29. J.P. Berenger, A perfectly matched layer for the absorption of electromagnetic waves, J Comput Phys 114 (1994), 185–200.

30. D. Gottlieb and S.A. Orszag, Numerical analysis of spectral methods: Theory and applications, Society for Industrial and Applied Mathematics, Philadelphia, 1993.

31. J. Shen, T. Tang, and L. Wang, Spectral methods: Algorithms, analysis and applications, Springer-Verlag, Berlin Heidelberg, 2011.

32. Z. Xu, X. Dong, and X. Zhao, On time-splitting pseudospectral discretization for nonlinear Klein-Gordon equation in nonrelativistic limit regime, Commun Comput Phys 16 (2014), 440–466.

33. W. Bao and Y. Cai, Mathematical theory and numerical methods for Bose-Einstein condensation, Kinet Relat Models 6 (2013), 1–135.

34. Ch. Lubich, On splitting methods for Schrödinger-Poisson and cubic nonlinear Schrödinger equations, Math Comput 77 (2008), 2141–2153.

35. L. Burden and J. Douglas, Numerical analysis, Thomson/Brooks/Cole, U.S., 2005.

36. B.G. Pachpatte, Inequalities for finite difference equations, Monographs and textbooks in pure and applied mathematics, Marcel Dekker, New York, 2002.

37. W. Bao and Y. Cai, Optimal error estimates of finite difference methods for the Gross-Pitaevskii equation with angular momentum rotation, Math Comput 82 (2013), 99–128.

38. T. Wang and X. Zhao, Optimal l^∞ error estimates of finite difference methods for the coupled Gross-Pitaevskii equations in high dimensions, Sci China Math 57 (2014), 2189–2214.

39. S. Klainerman and M. Machedon, Space-time estimates for null forms and the local existence theorem, Commun Pure Appl Math 46 (1993), 1221–1268.

40. V. Grimm, On error bounds for the Gautschi-type exponential integrator applied to oscillatory second-order differential equations, Numer Math 100 (2005), 71–89.